ELECTRONIC SUPPORTING INFORMATION

for

Building a functionalizable, potent chemiluminescent agent: A rational design study on 6,8-substituted luminol derivatives

by

Theodoros Mikroulis,[a] M. Consuelo Cuquerella,[b] Angelo Giussani,[c] Anna Pantelia,[a] Gemma M. Rodríguez-Muñiz,[b] Georgios Rotas,[a] Daniel Roca-Sanjuán,*[c] Miguel A. Miranda,*[b] and Georgios C. Vougioukalakis,*[a]

[a] Laboratory of Organic Chemistry, Department of Chemistry, National and Kapodistrian University of Athens, Panepistimiopolis, 15771 Athens, Greece, E-mail: vougiouk@chem.uoa.gr

[b] Instituto de Tecnología Química UPV-CSIC, Universitat Politècnica de València, Camino de Vera s / n, 46022 València, Spain, Email: mmiranda@qim.upv.es

[c] Instituto de Ciencia Molecular, Universitat de València, P.O. Box 22085, 46071 València, Spain, Email: daniel.roca@uv.es

Table of contents

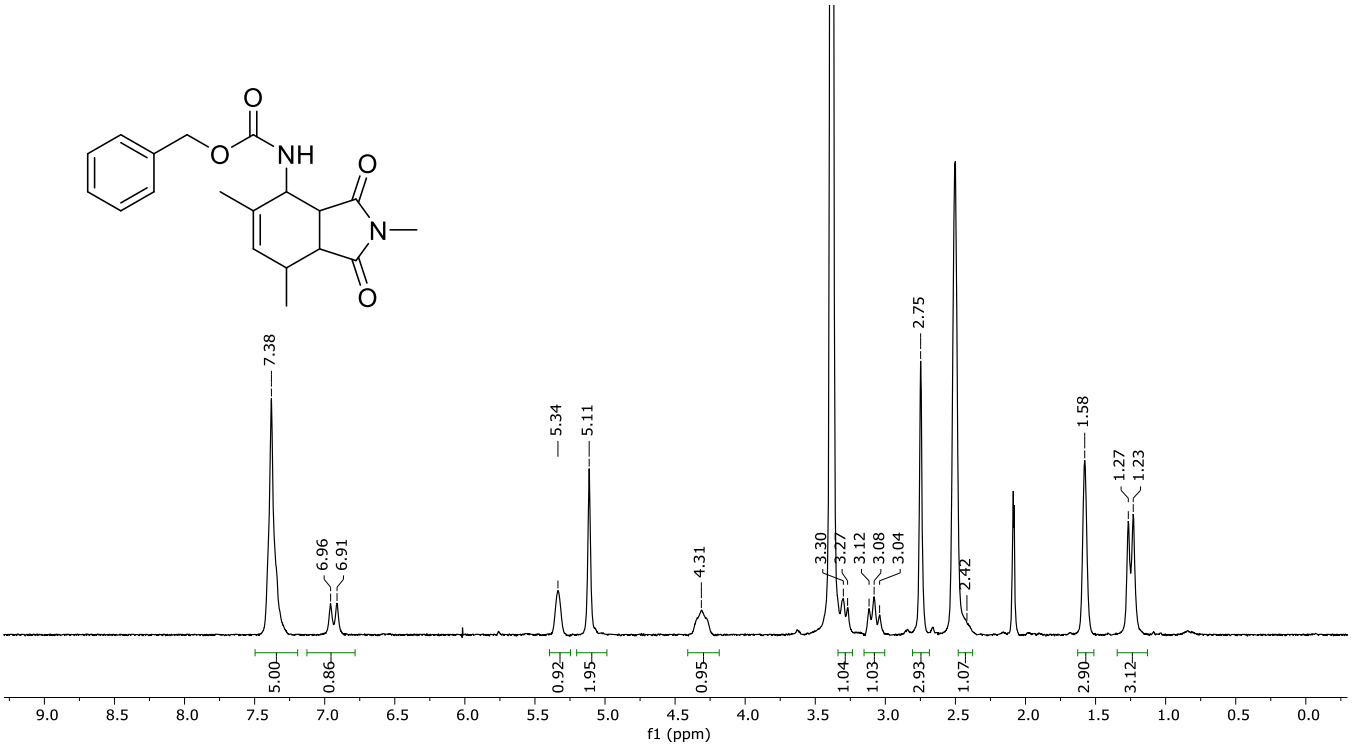

Figure S3. 1H-NMR (200 MHz, DMSO-d_6) spectrum of **1.**

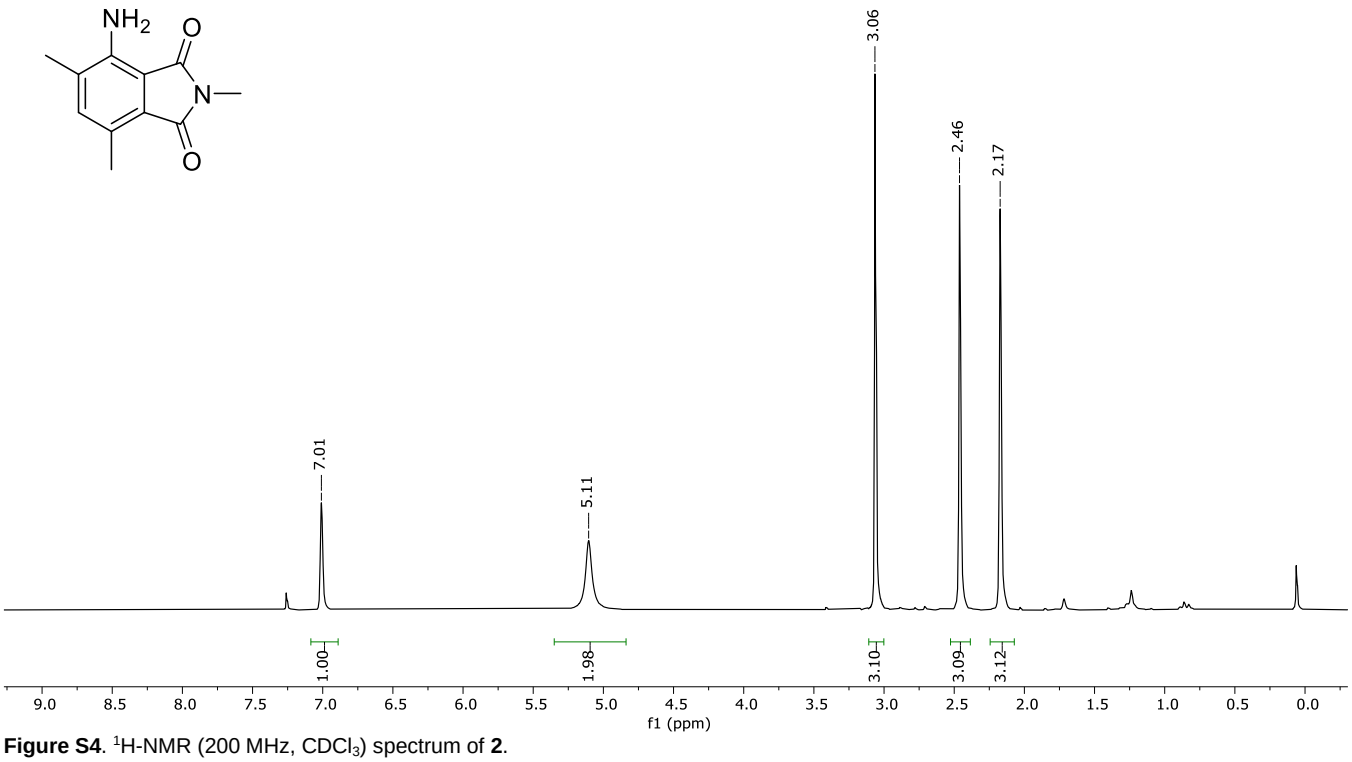

Figure S4. ^{1}H-NMR (200 MHz, $CDCl_3$) spectrum of **2**.

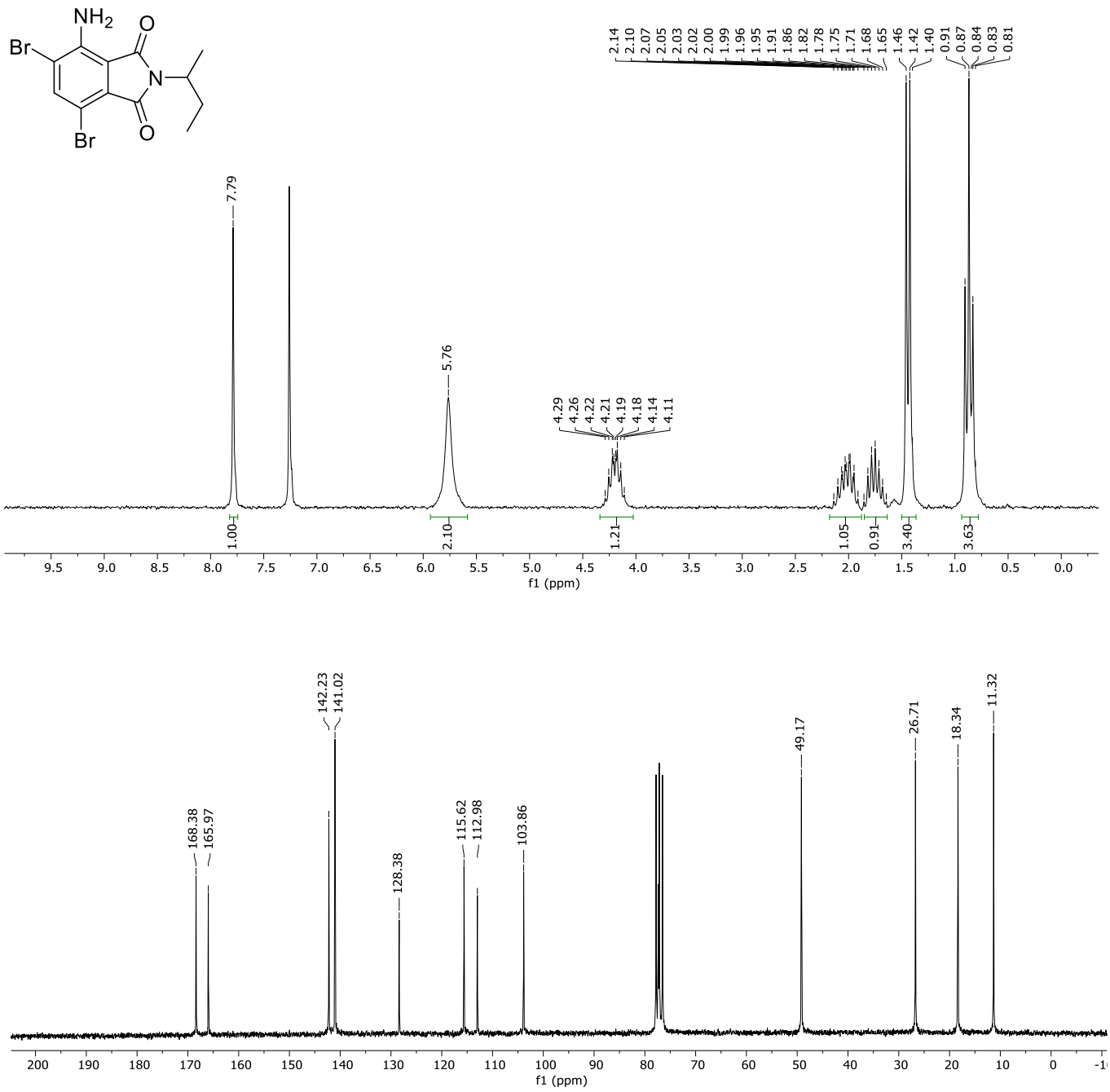

Figure S3. ^{1}H (200 MHz, up) and ^{13}C (50 MHz, down) NMR ($CDCl_3$) spectra of **4**.

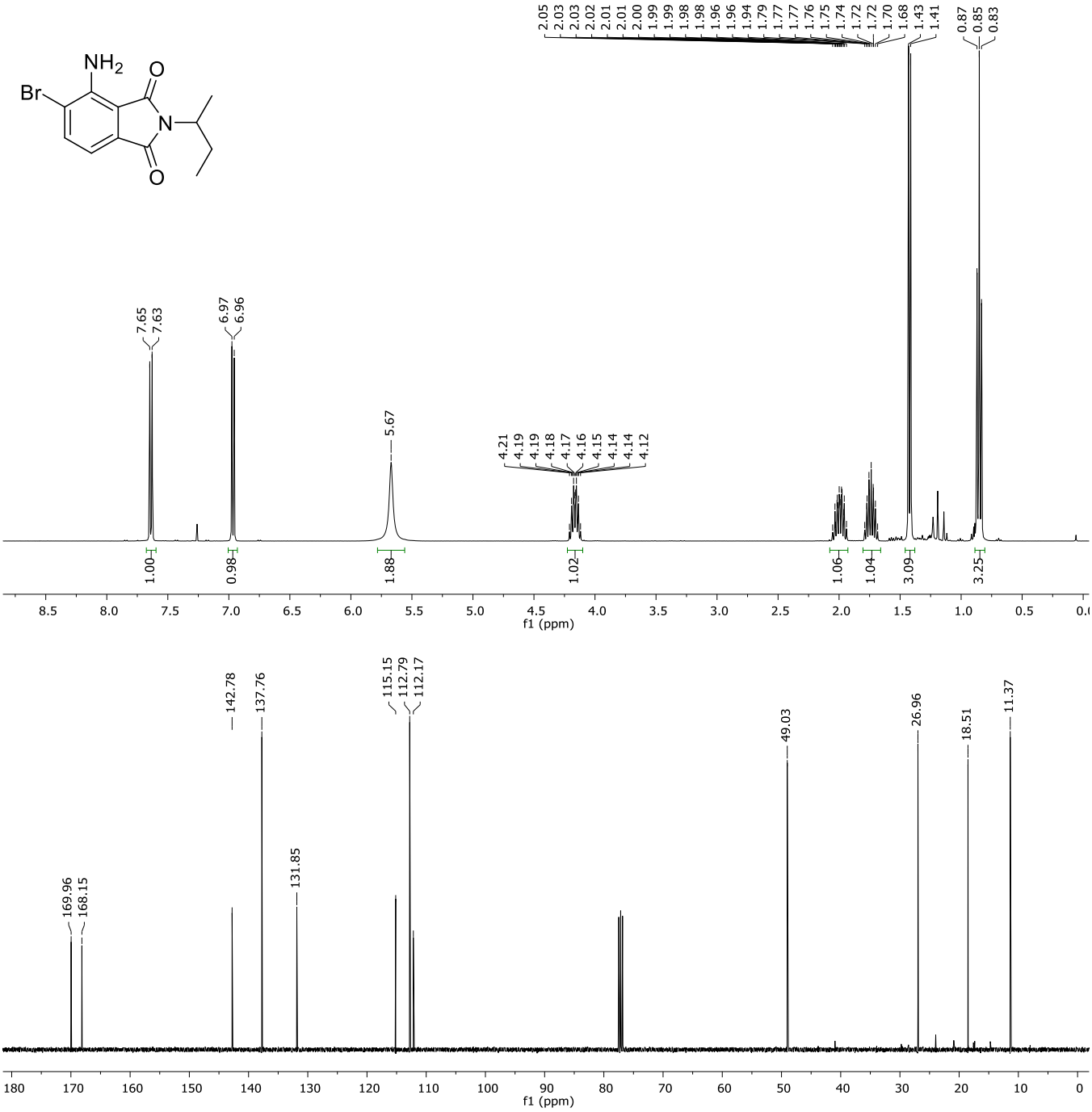

Figure S4. ^{1}H (400 MHz, up) and ^{13}C (101 MHz, down) NMR ($CDCl_3$) spectra of **6a**.

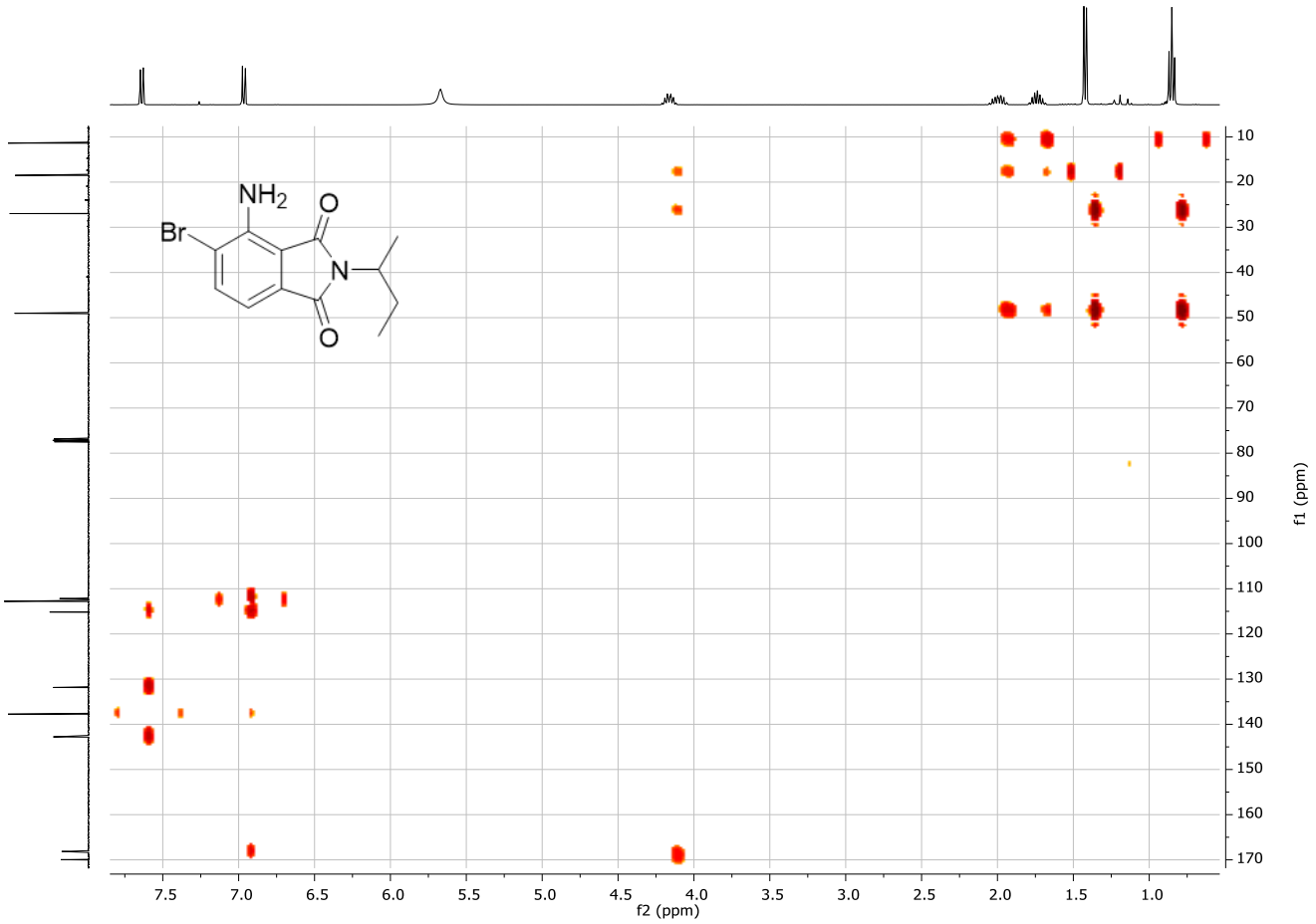

Figure S5. 2D (^{1}H, ^{13}C) HMBC NMR ($CDCl_3$) correlation of **6a**.

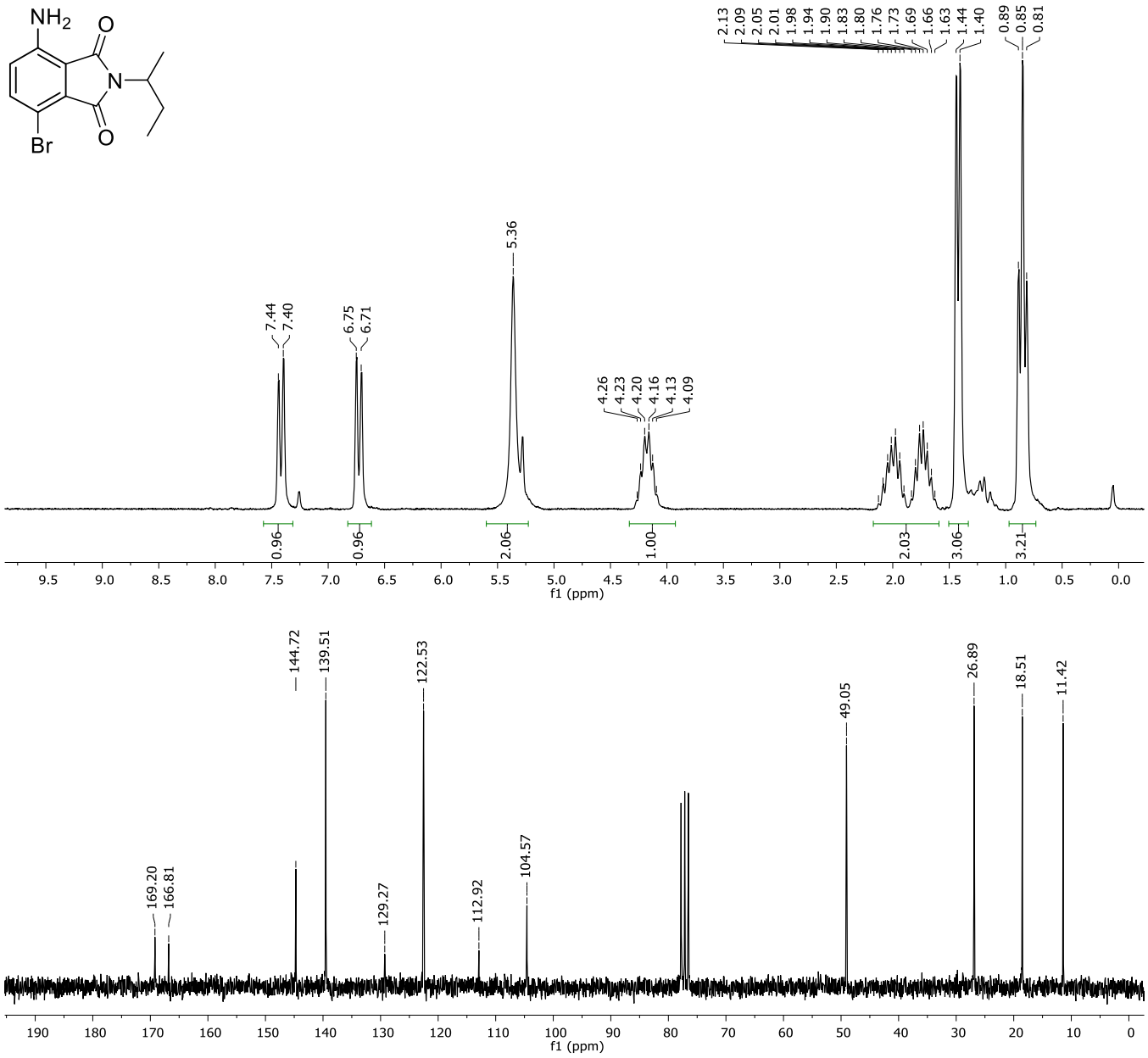

Figure S6. ^{1}H (200 MHz, up) and ^{13}C (50 MHz, down) NMR ($CDCl_3$) spectra of **6b**.

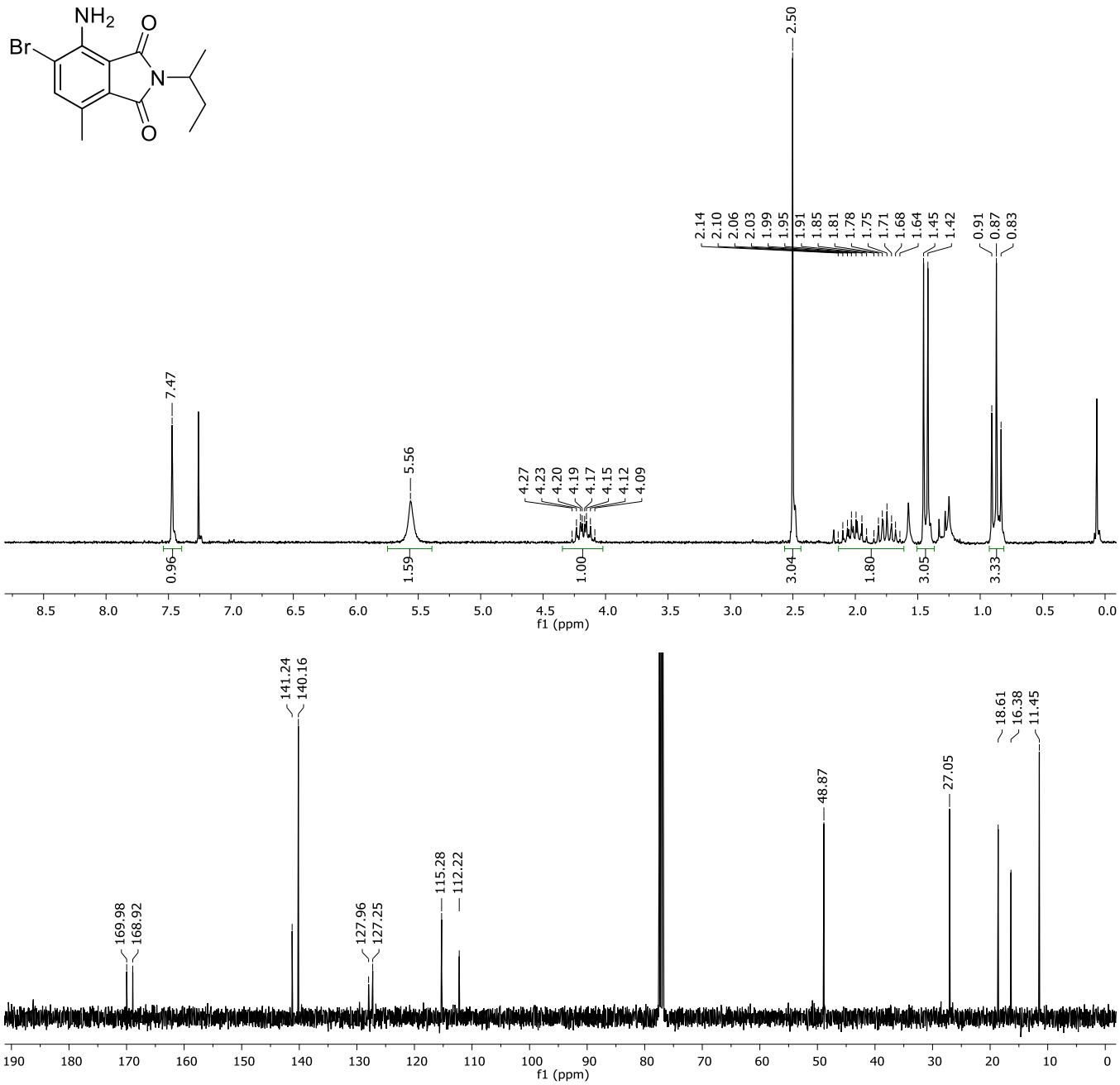

Figure S7. ^{1}H (200 MHz, up) and ^{13}C (50 MHz, down) NMR ($CDCl_3$) spectra of **7a**.

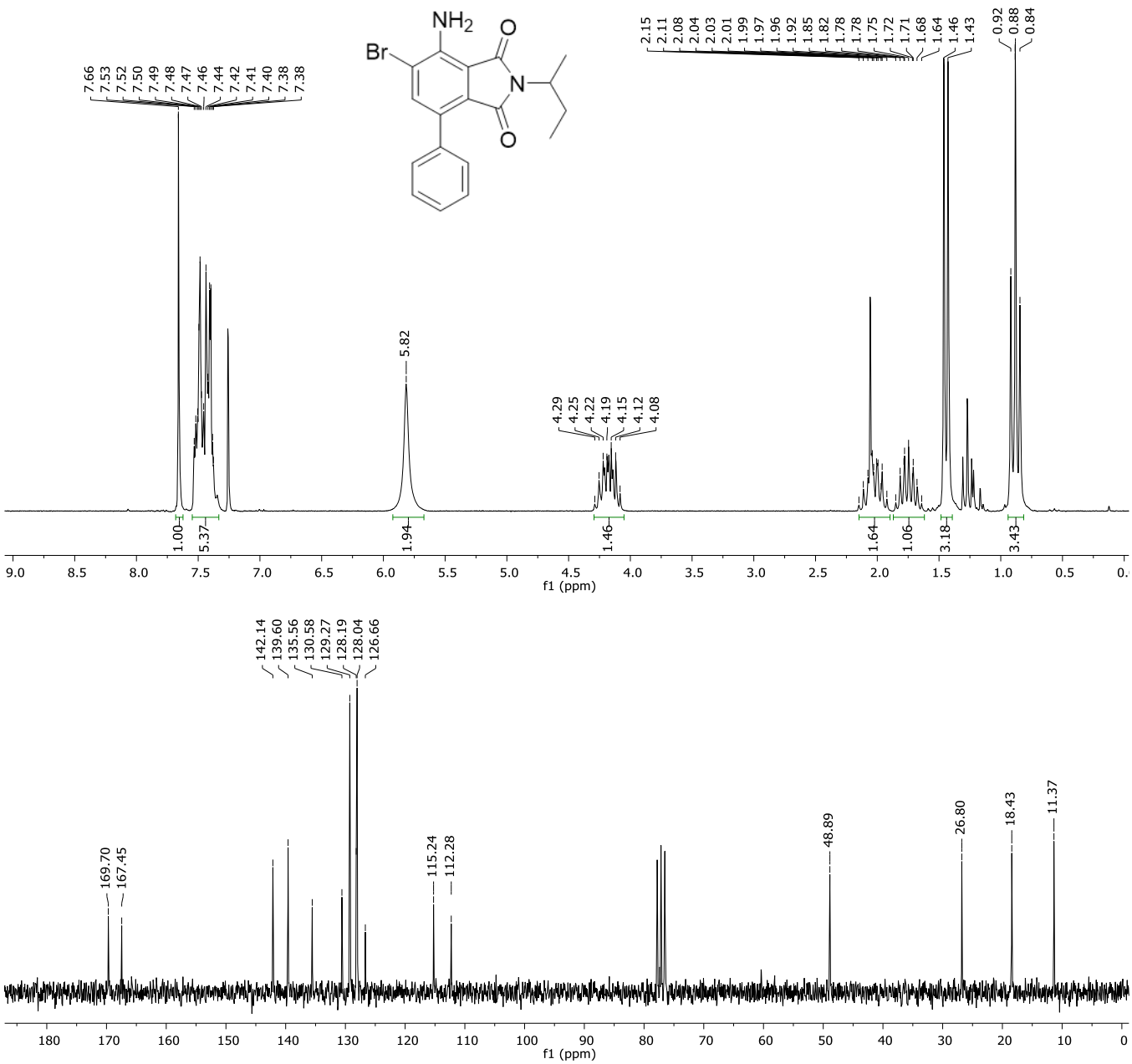

Figure S8. ^{1}H (200 MHz, up) and ^{13}C (50 MHz, down) NMR ($CDCl_3$) spectra of **7b**.

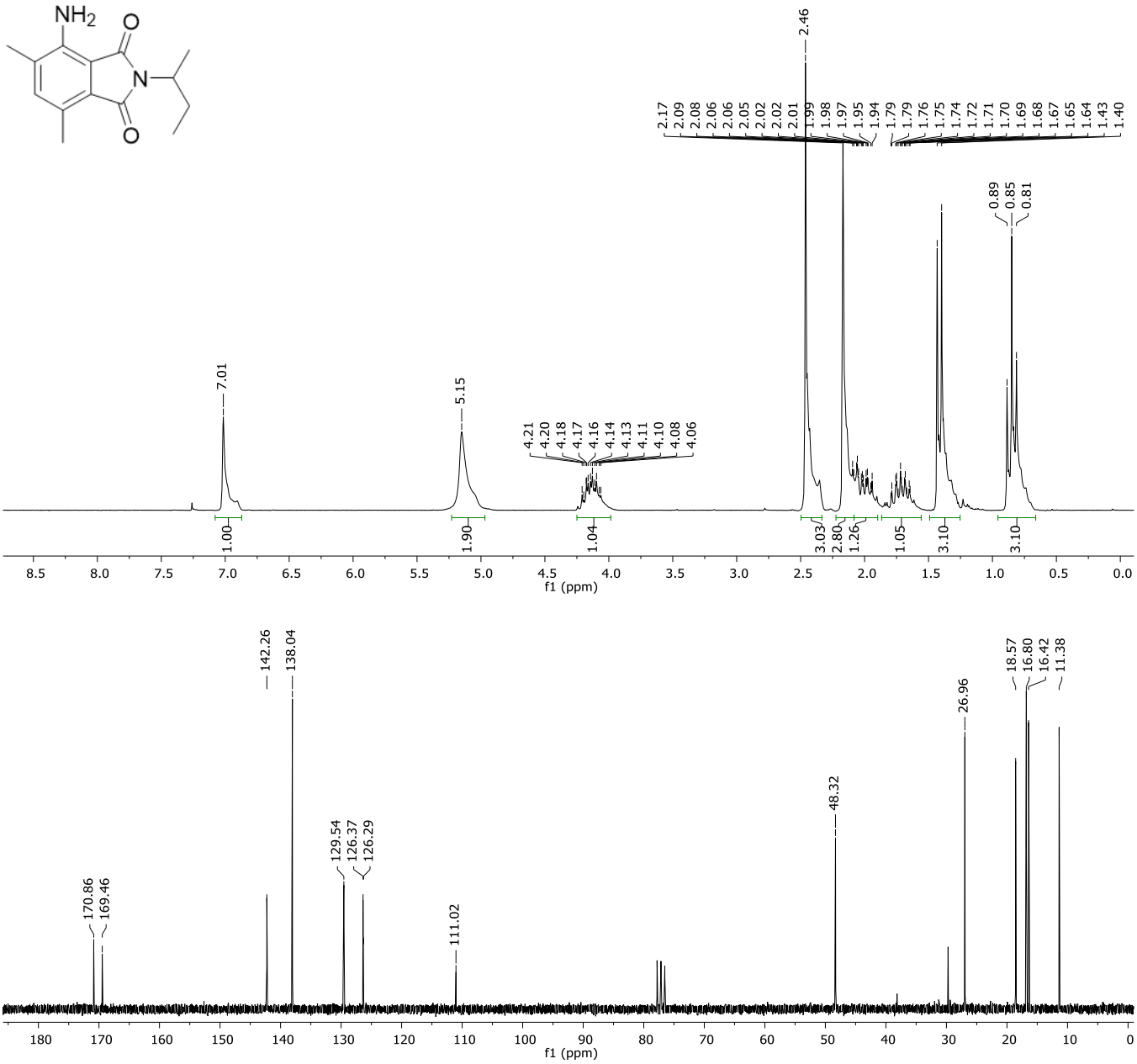

Figure S9. ^{1}H (200 MHz, up) and ^{13}C (50 MHz, down) NMR ($CDCl_3$) spectra of **5a**.

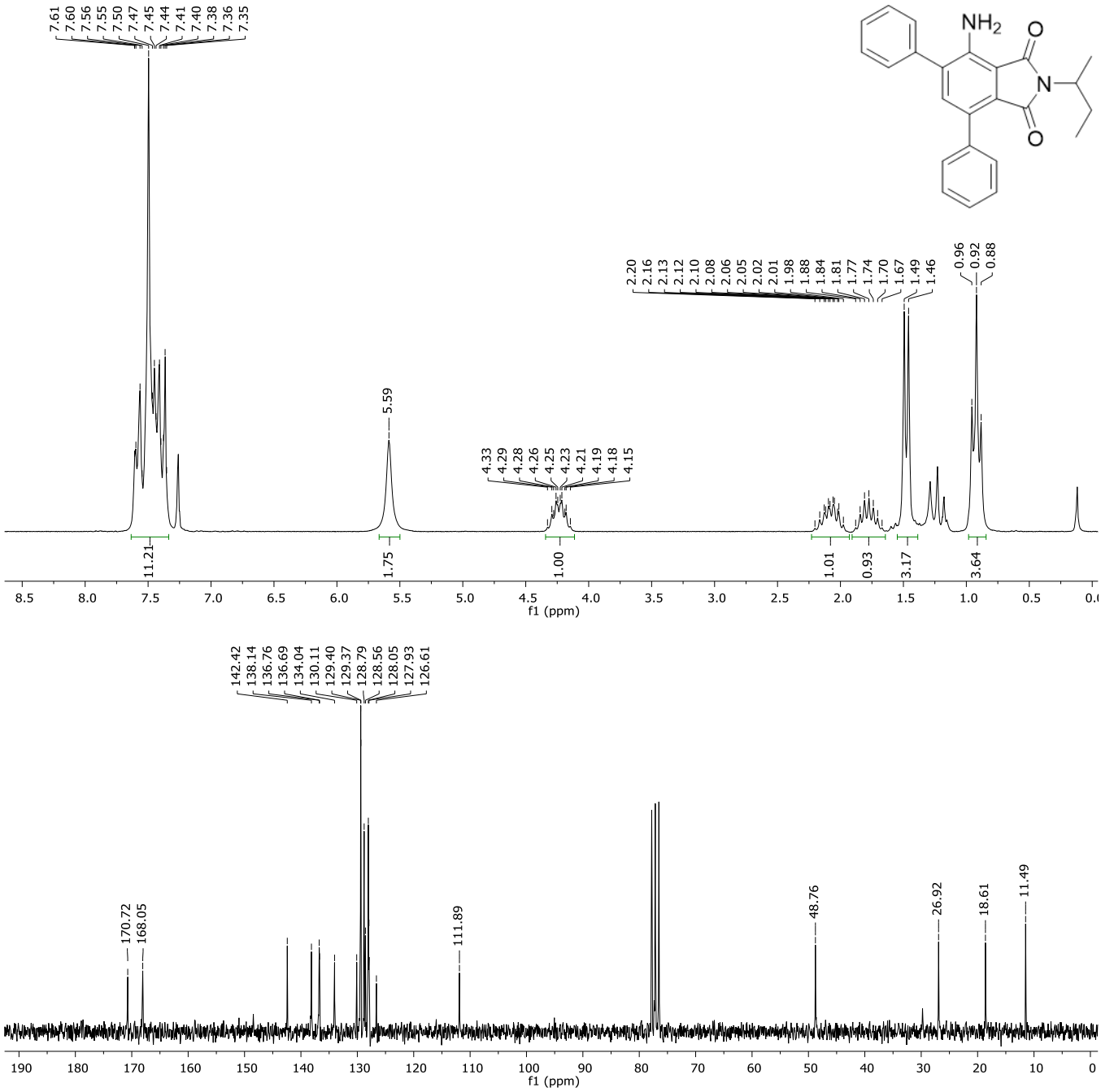

Figure S10. ^{1}H (200 MHz, up) and ^{13}C (50 MHz, down) NMR ($CDCl_3$) spectra of **5b**.

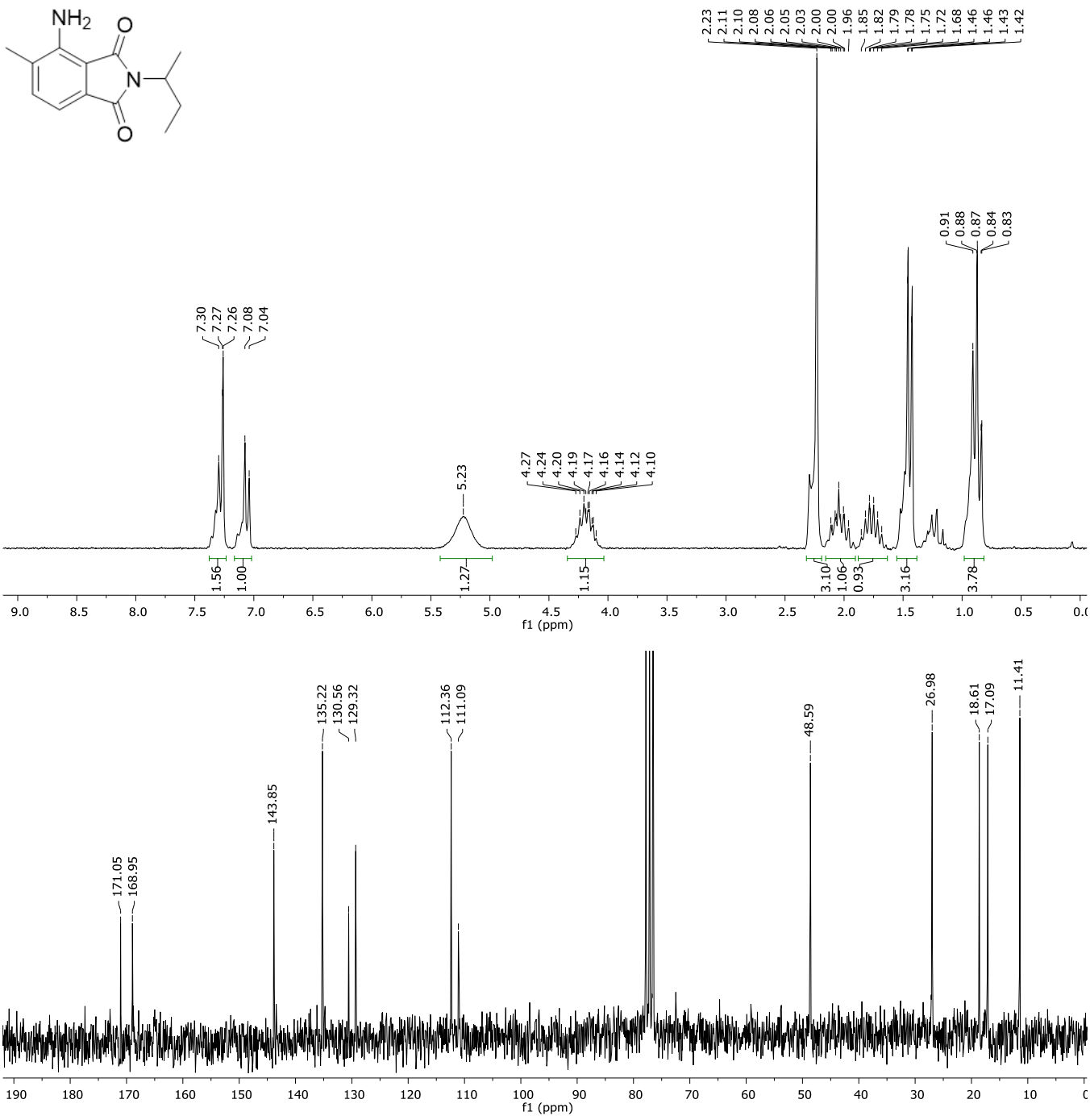

Figure S11. ^{1}H (200 MHz, up) and ^{13}C (50 MHz, down) NMR ($CDCl_3$) spectra of **5c**.

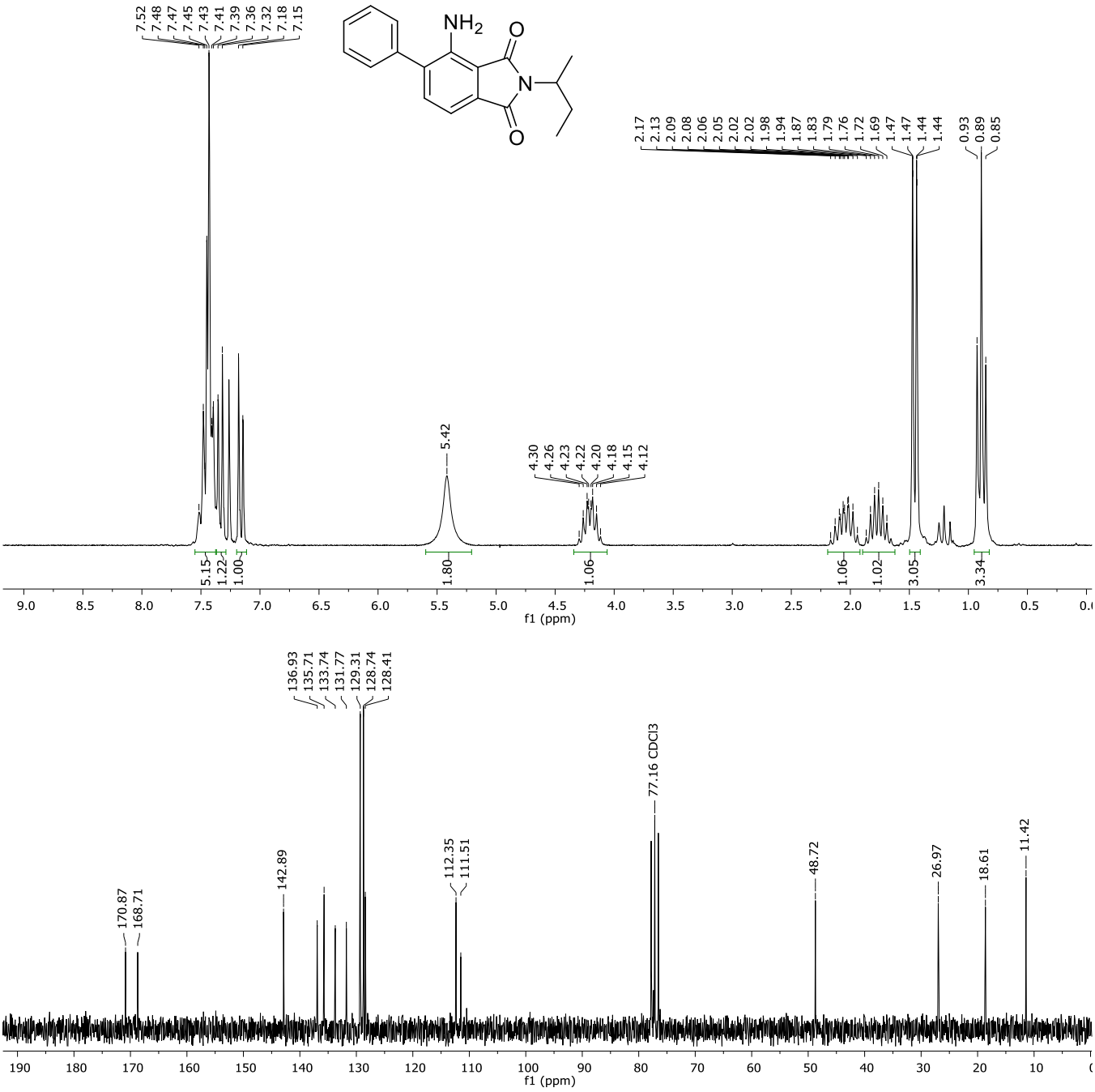

Figure S12. ^{1}H (200 MHz, up) and ^{13}C (50 MHz, down) NMR ($CDCl_3$) spectra of **5d**.

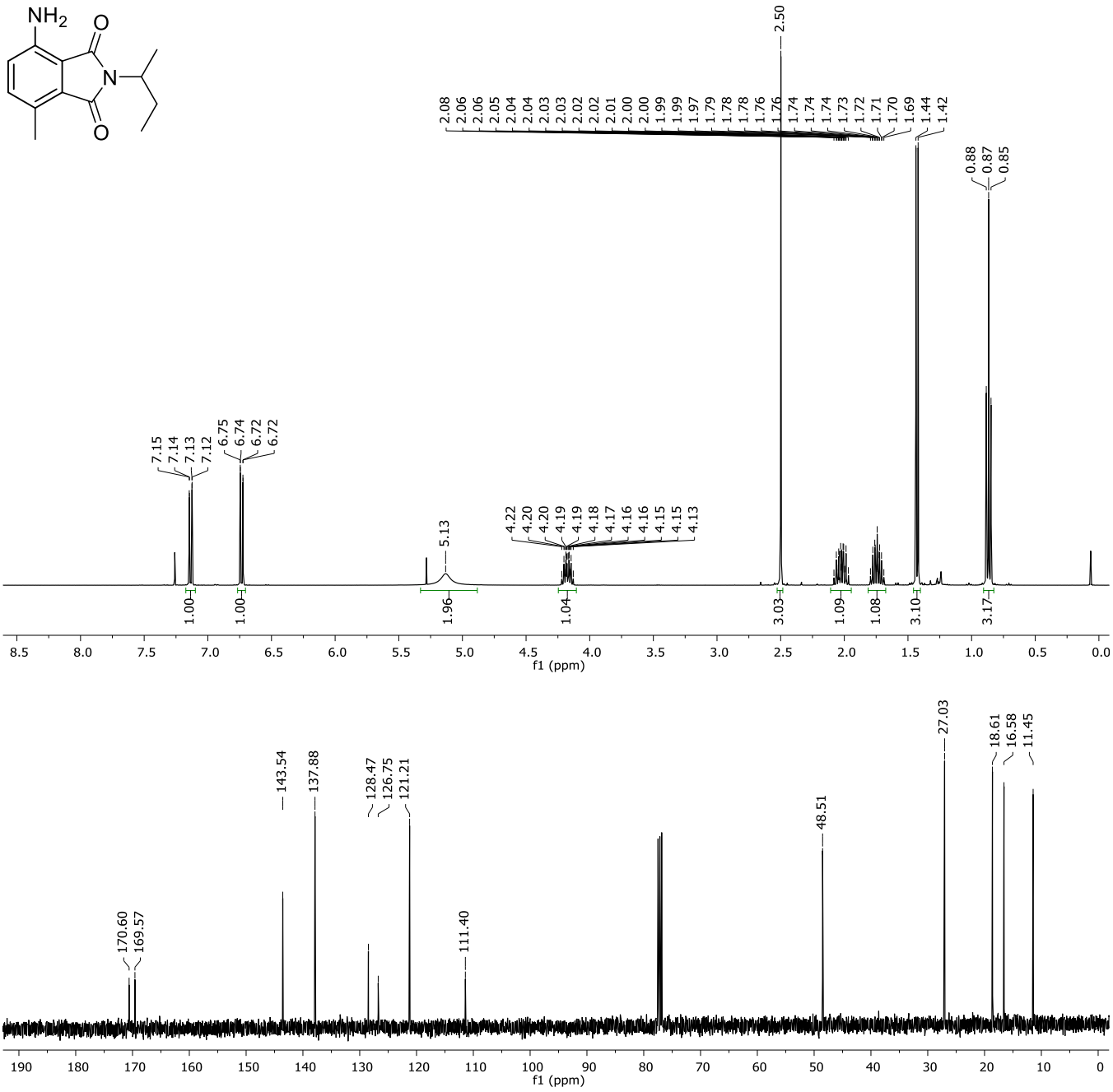

Figure S13. ^{1}H (400 MHz, up) and ^{13}C (100 MHz, down) NMR ($CDCl_3$) spectra of **5e**.

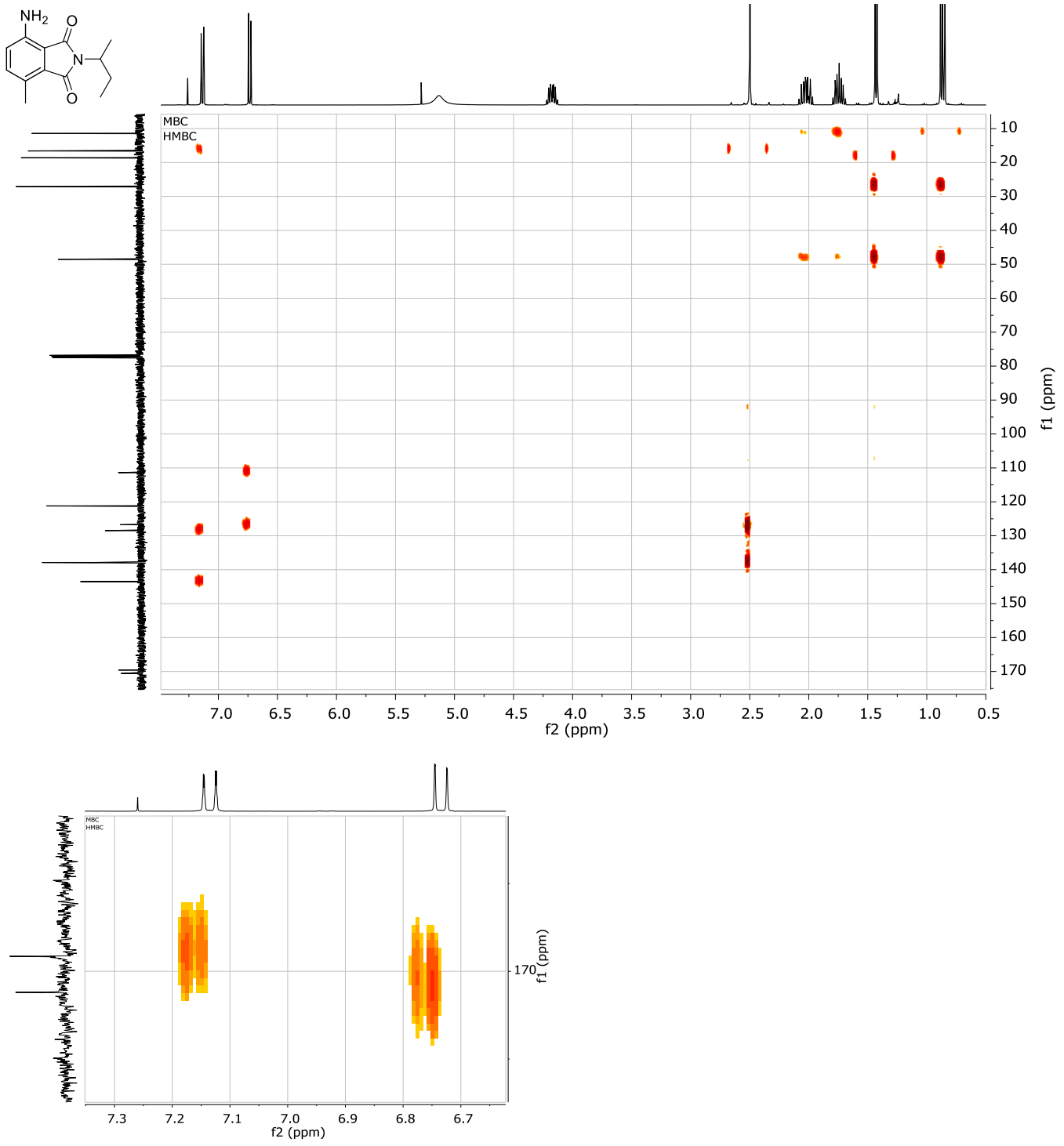

Figure S14. 2D (^{1}H,^{13}C)-HMBC NMR ($CDCl_3$) correlation of **5e**. Down: magnification.

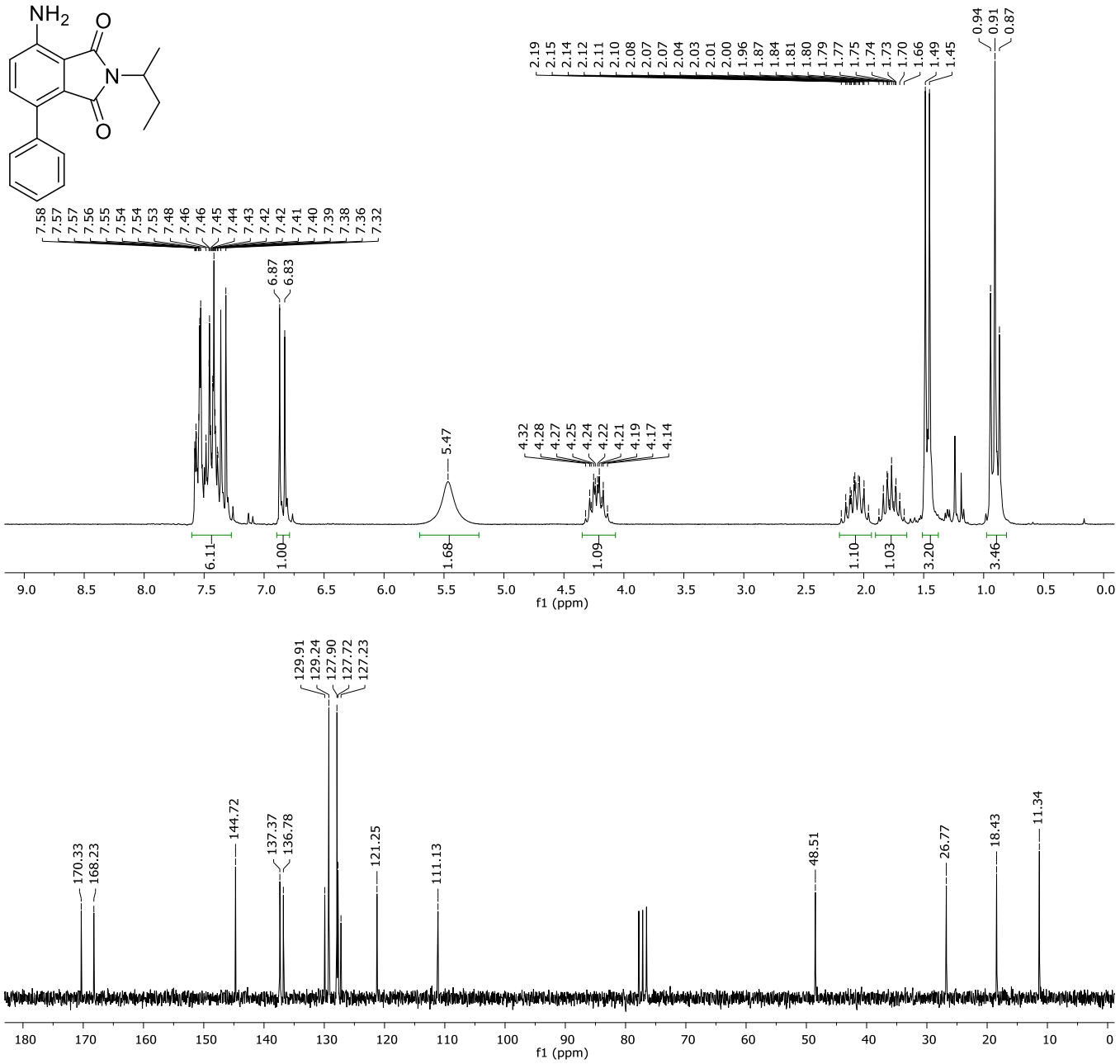

Figure S15. ^{1}H (200 MHz, up) and ^{13}C (50 MHz, down) NMR ($CDCl_3$) spectra of **5f**.

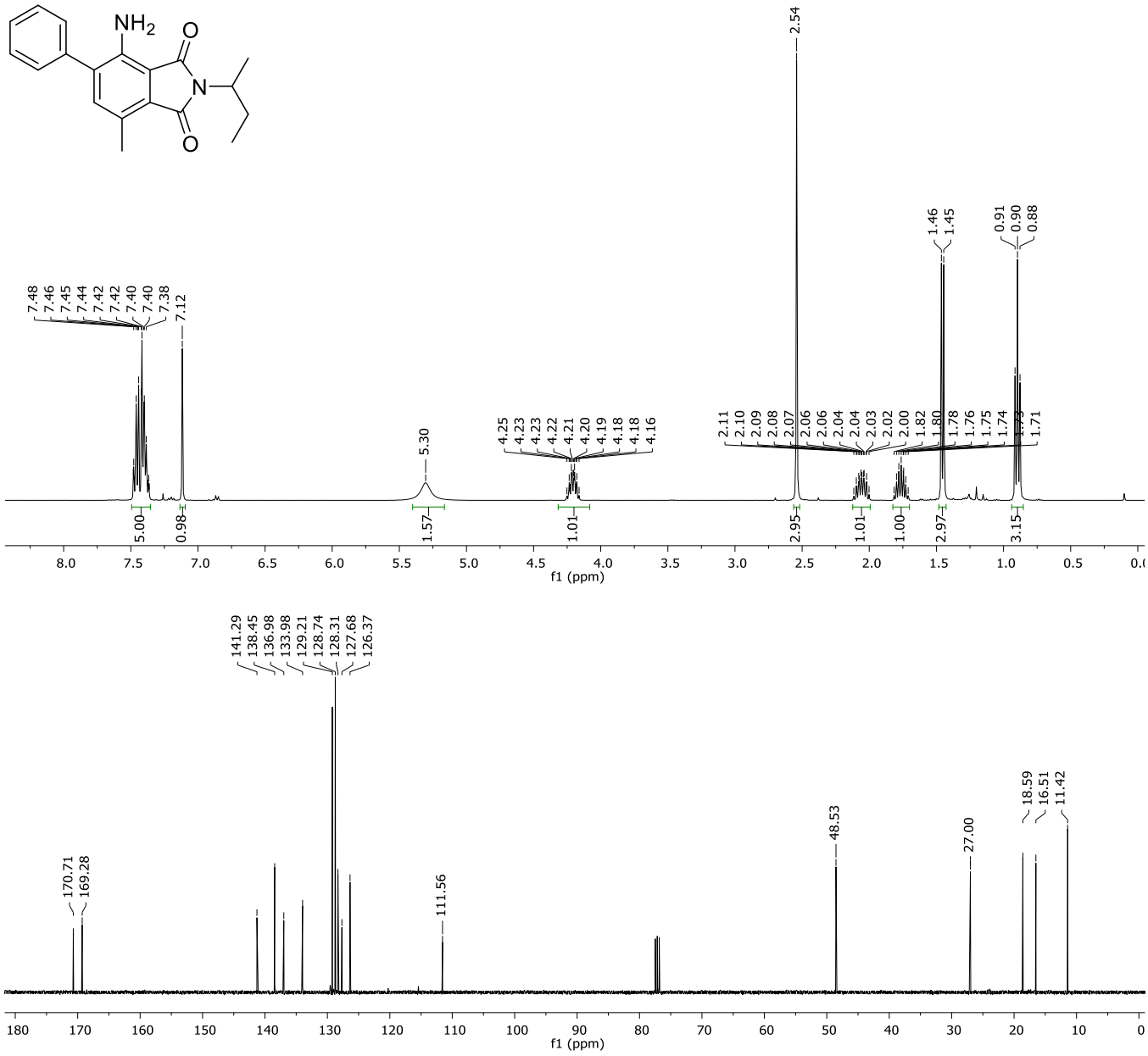

Figure S16. ^{1}H (400 MHz, up) and ^{13}C (100 MHz, down) NMR ($CDCl_3$) spectra of **5g**.

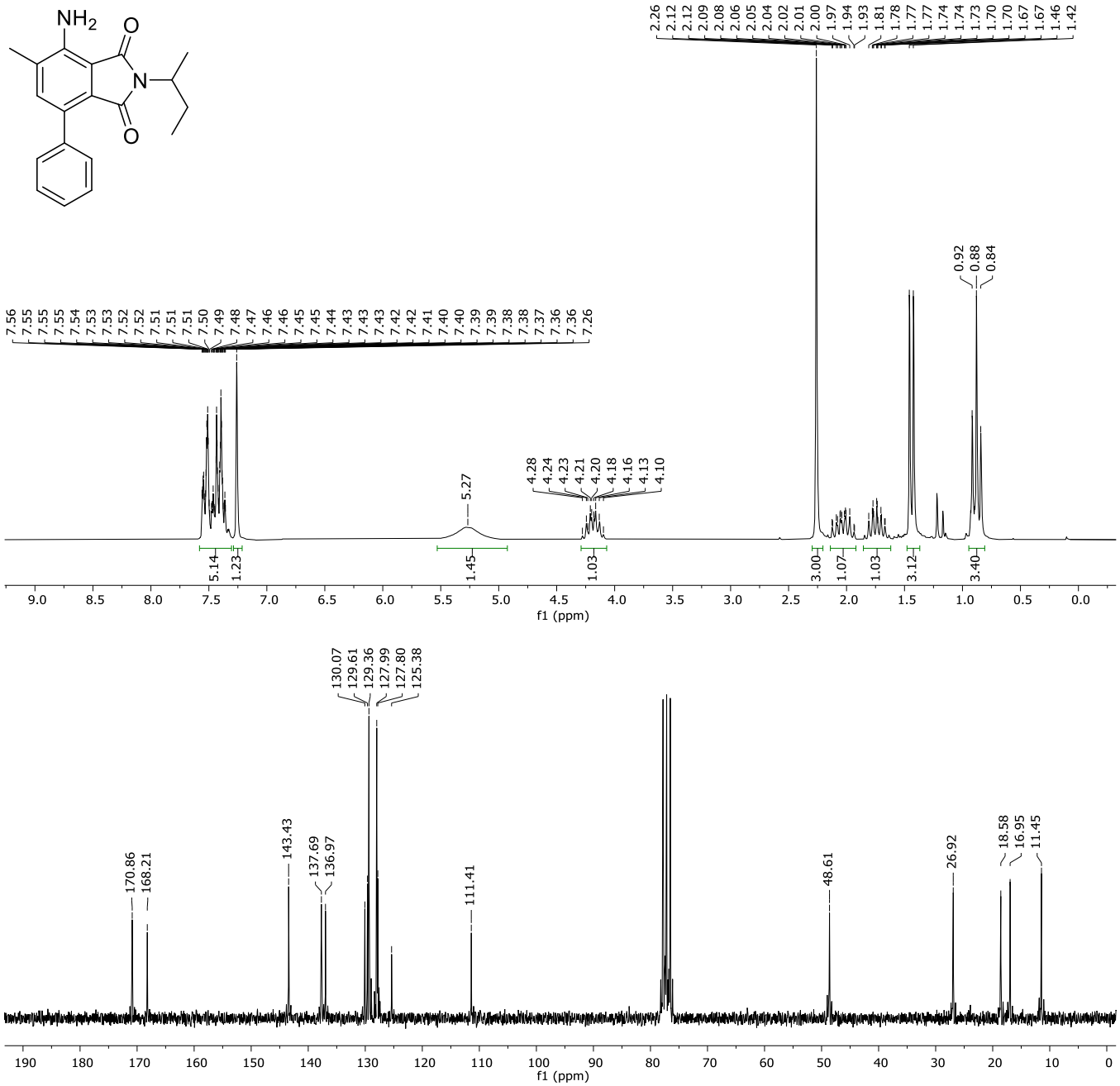

Figure S17. ^{1}H (200 MHz, up) and ^{13}C (50 MHz, down) NMR ($CDCl_3$) spectra of **5h**.

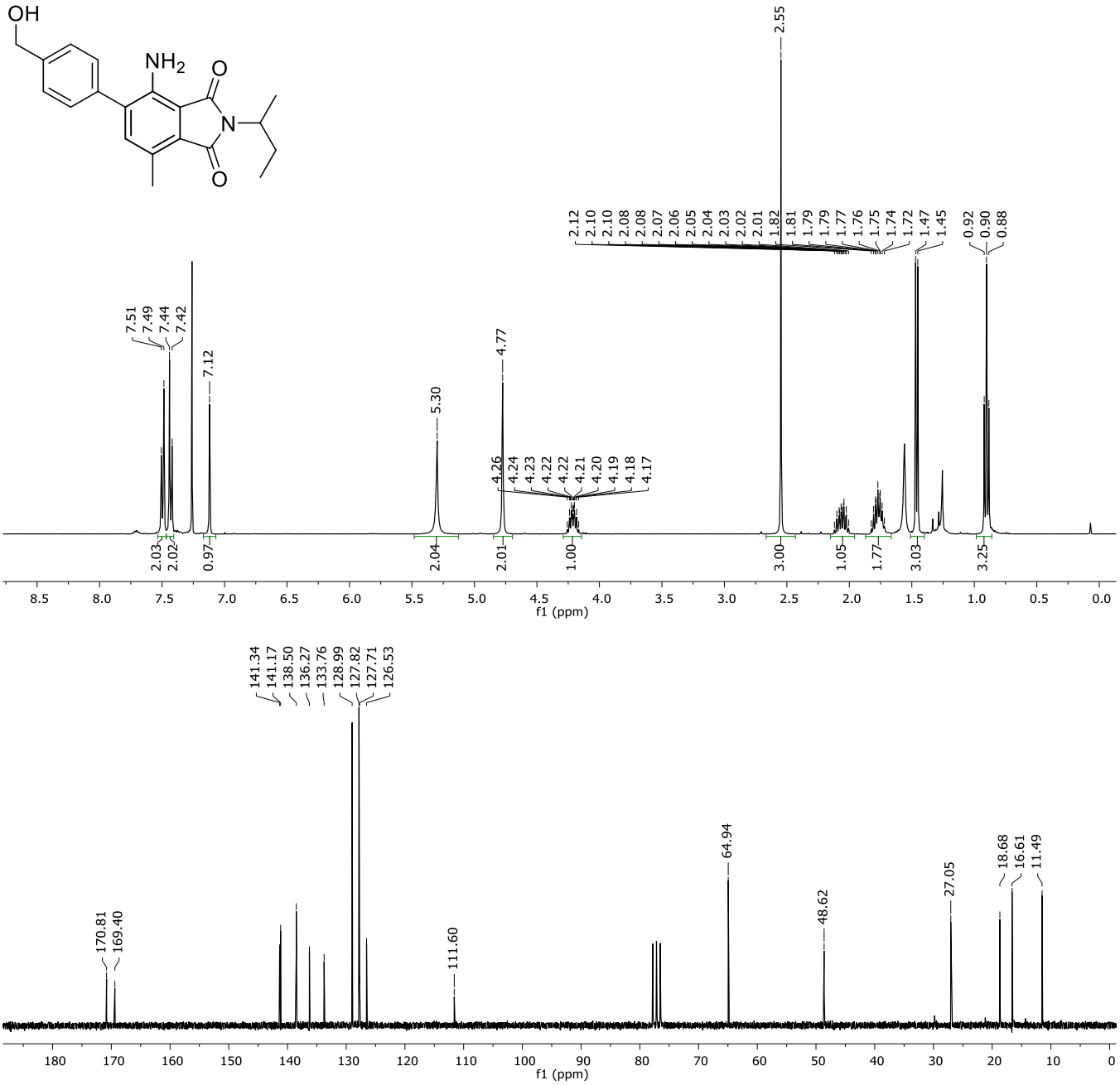

Figure S18. ^{1}H (400 MHz, up) and ^{13}C (100 MHz, down) NMR ($CDCl_3$) spectra of **5i**.

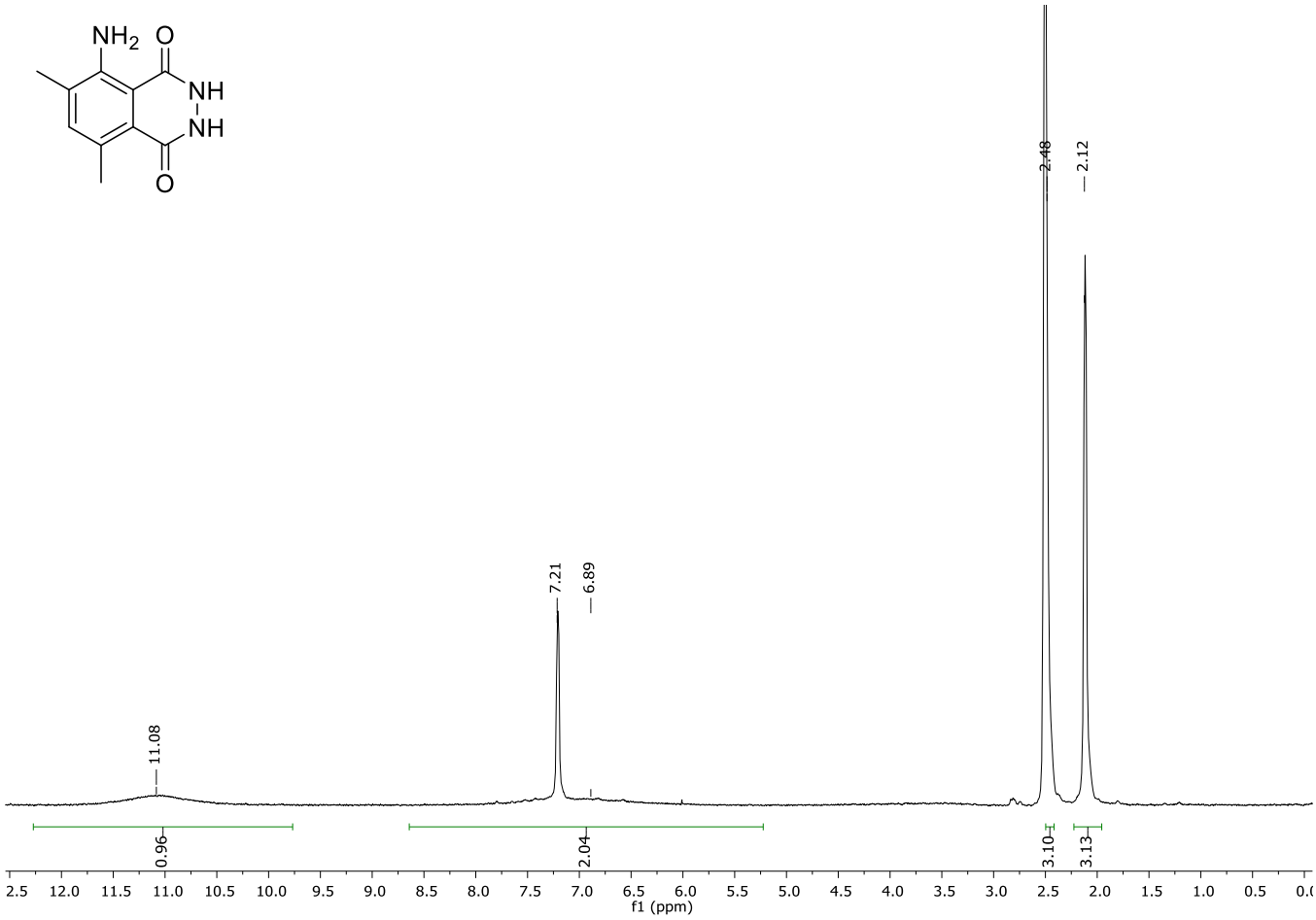

Figure S19. ^{1}H NMR (200 MHz, DMSO-d_6) spectrum of **8a**

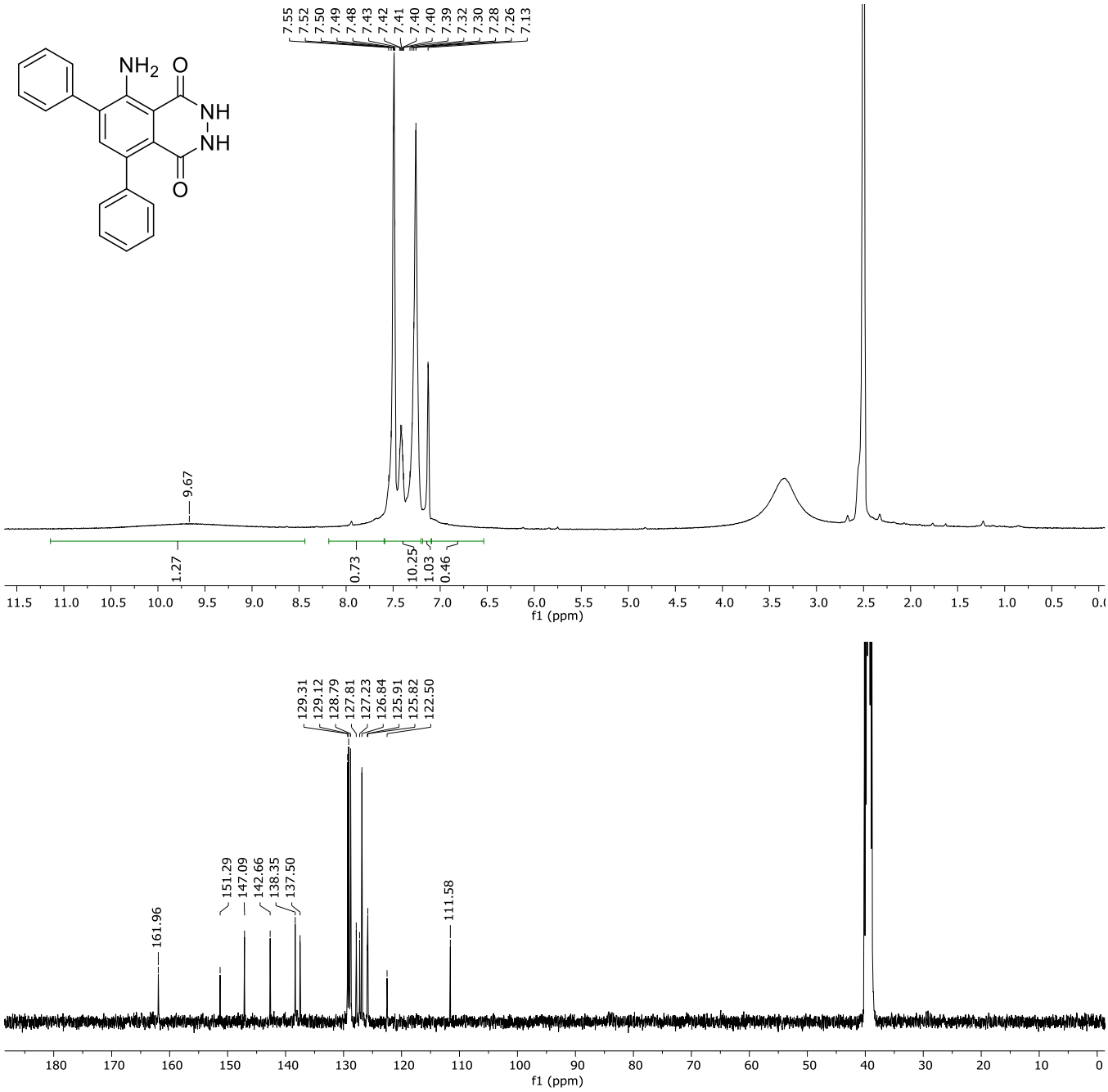

Figure S20. ^{1}H (400 MHz, up) and ^{13}C (100 MHz, down) NMR (DMSO-d_6) spectra of **8b**.

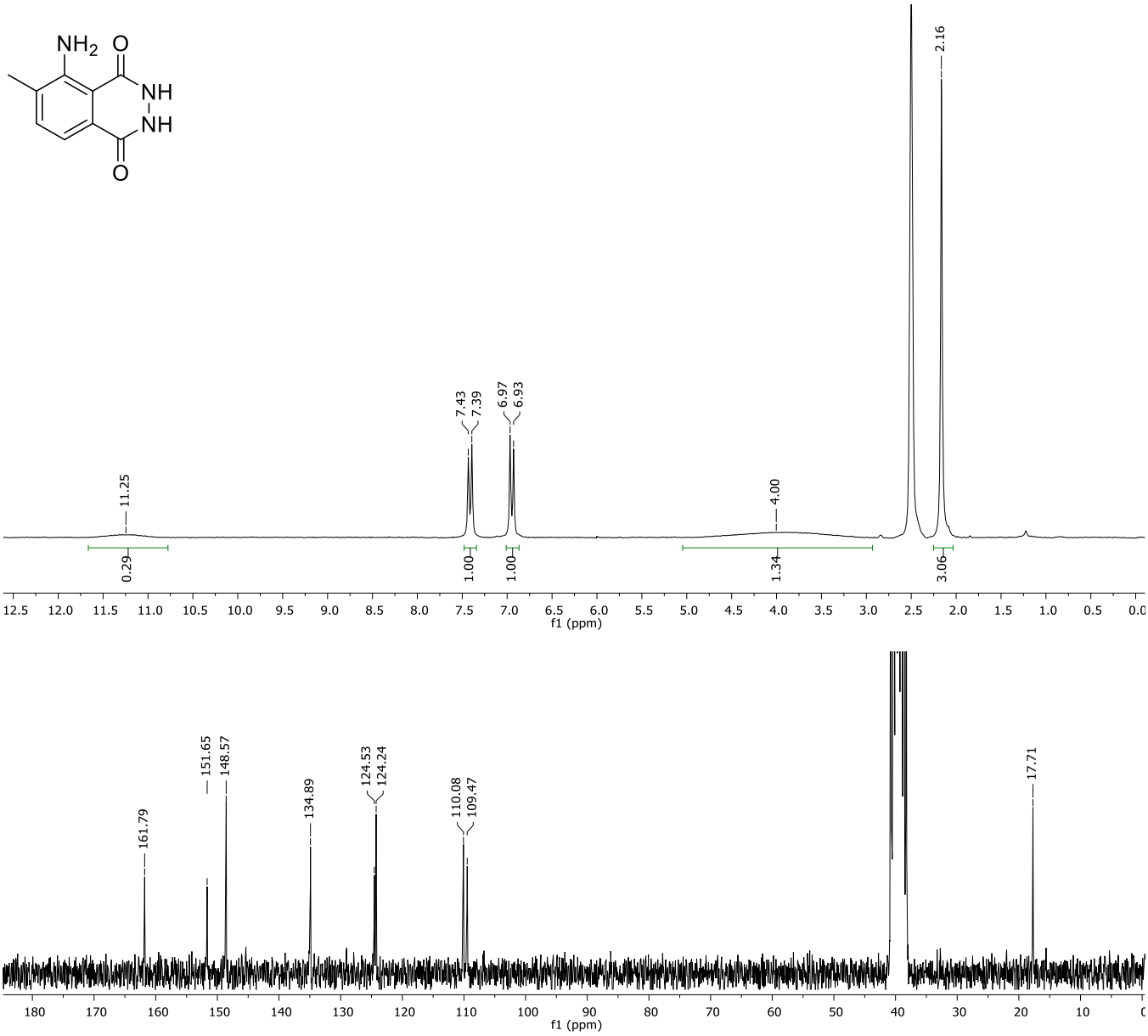

Figure S21. ^{1}H (200 MHz, up) and ^{13}C (50 MHz, down) NMR (DMSO-d_6) spectra of **8c**.

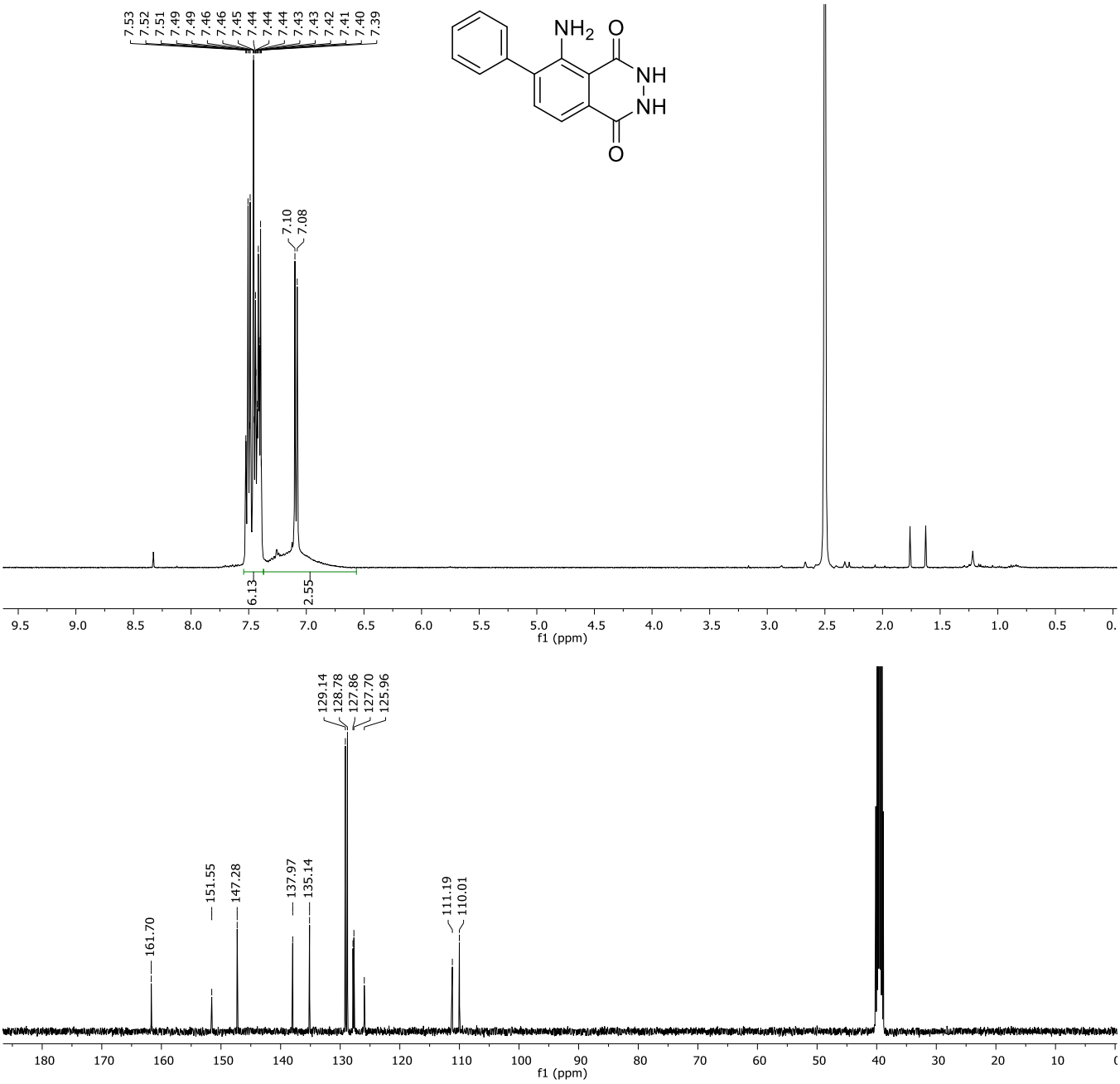

Figure S22. ^{1}H (400 MHz, up) and ^{13}C (100 MHz, down) NMR (DMSO-d_6) spectra of **8d**.

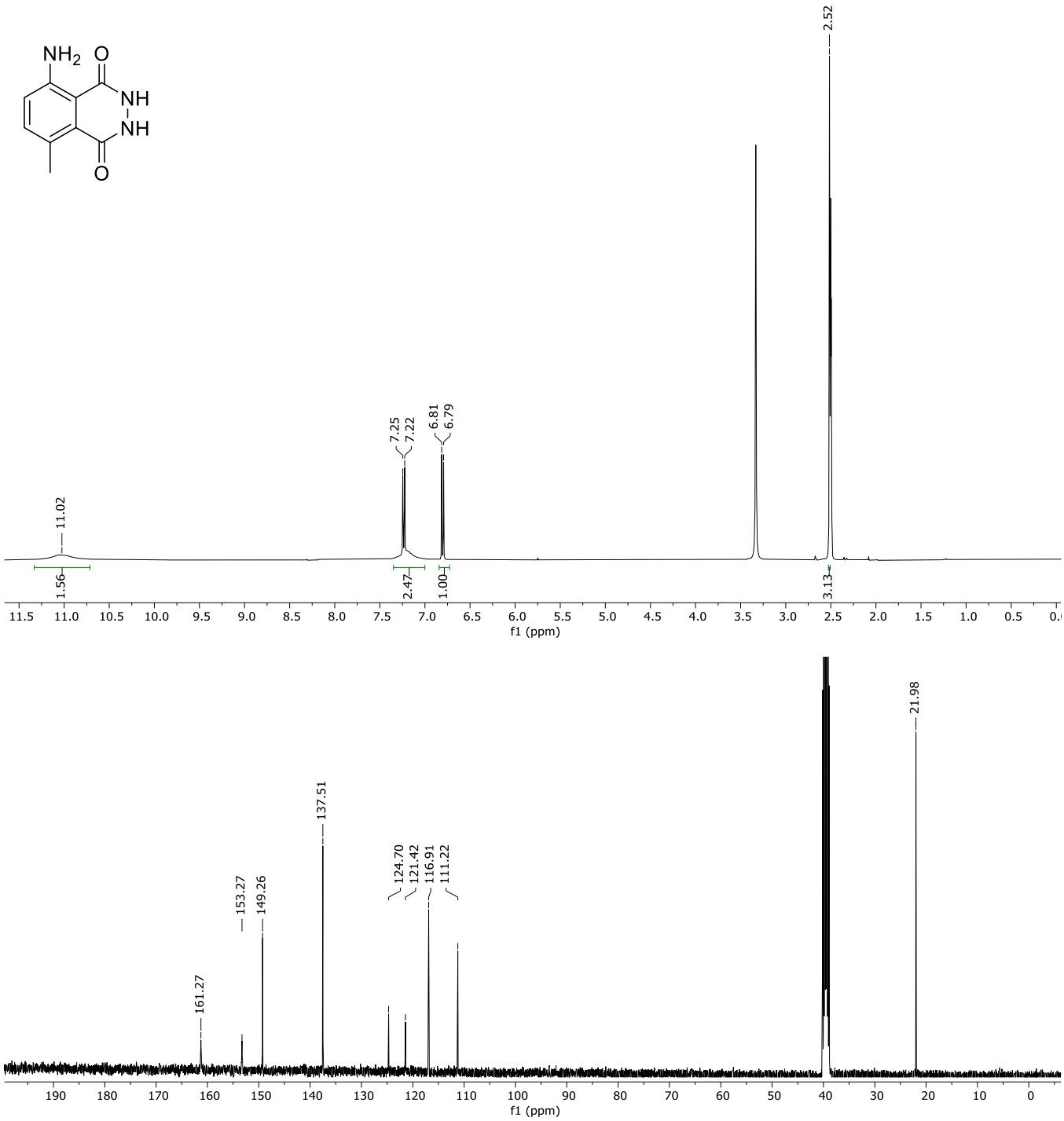

Figure S23. ^{1}H (400 MHz, up) and ^{13}C (100 MHz, down) NMR (DMSO-d_6) spectra of **8e**.

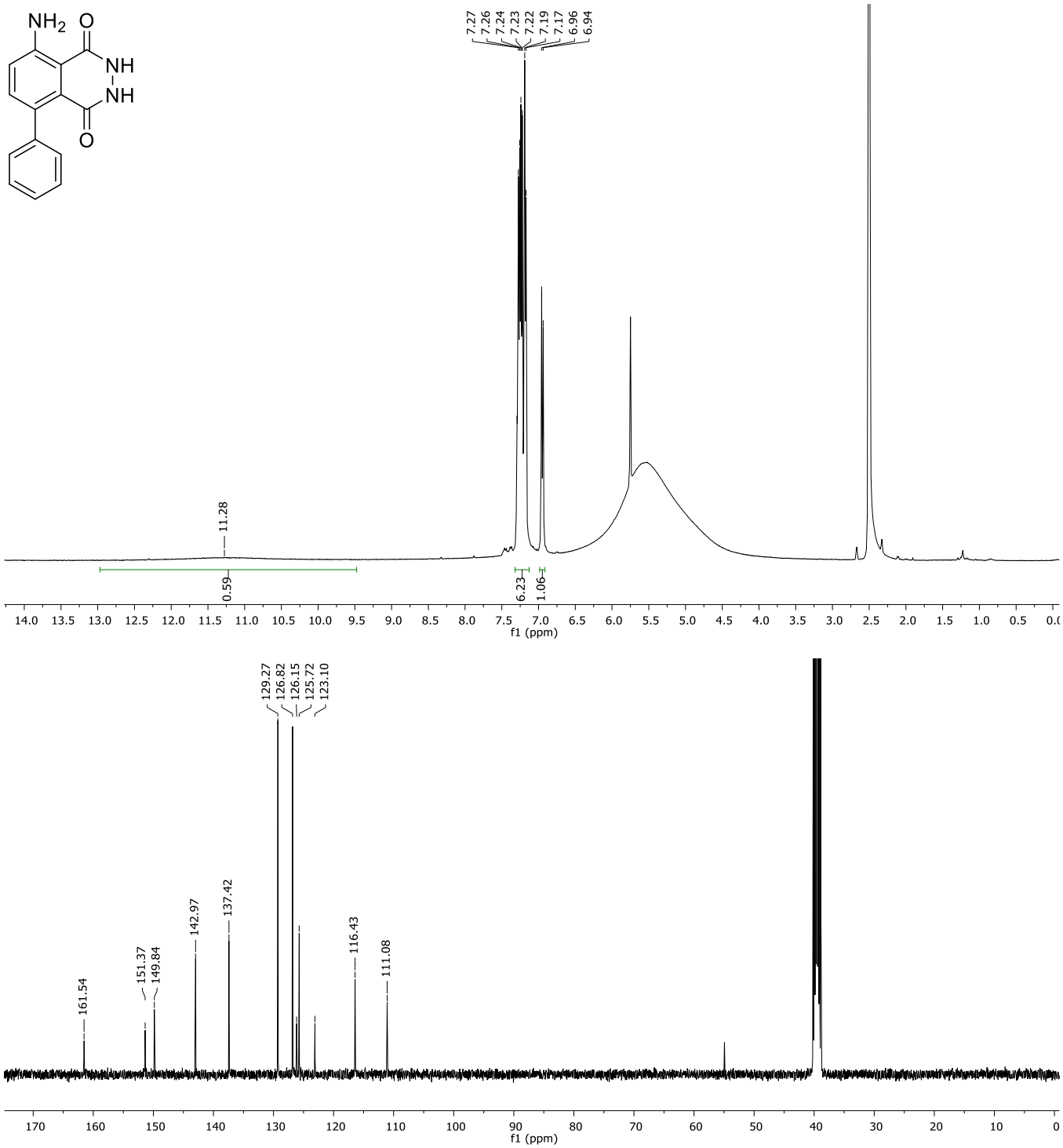

Figure S24. ^{1}H (400 MHz, up) and ^{13}C (100 MHz, down) NMR (DMSO-d_6) spectra of **8f**.

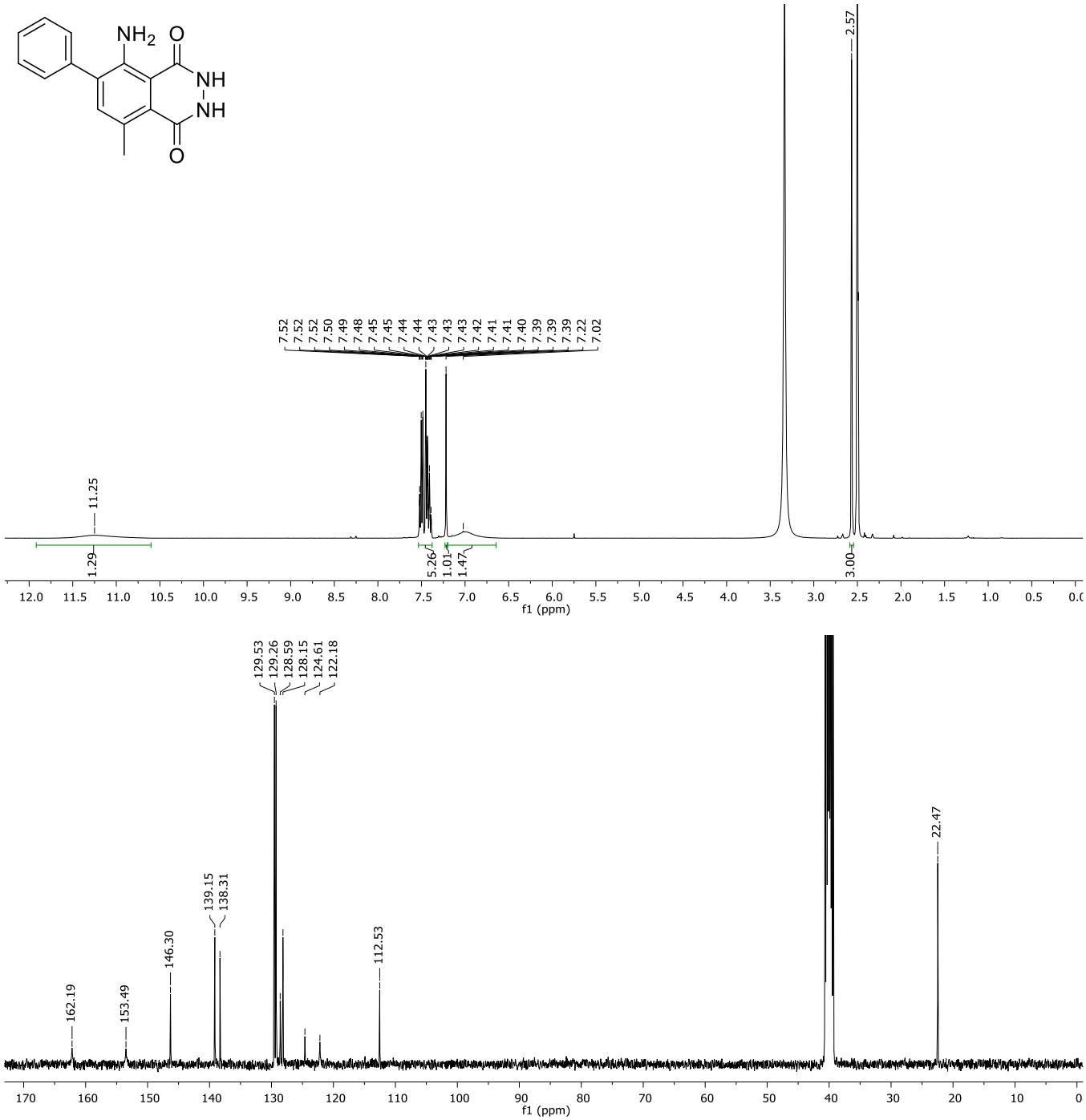

Figure S25. ^{1}H (400 MHz, up) and ^{13}C (101 MHz, down) NMR (DMSO-d_6) spectra of **8g**.

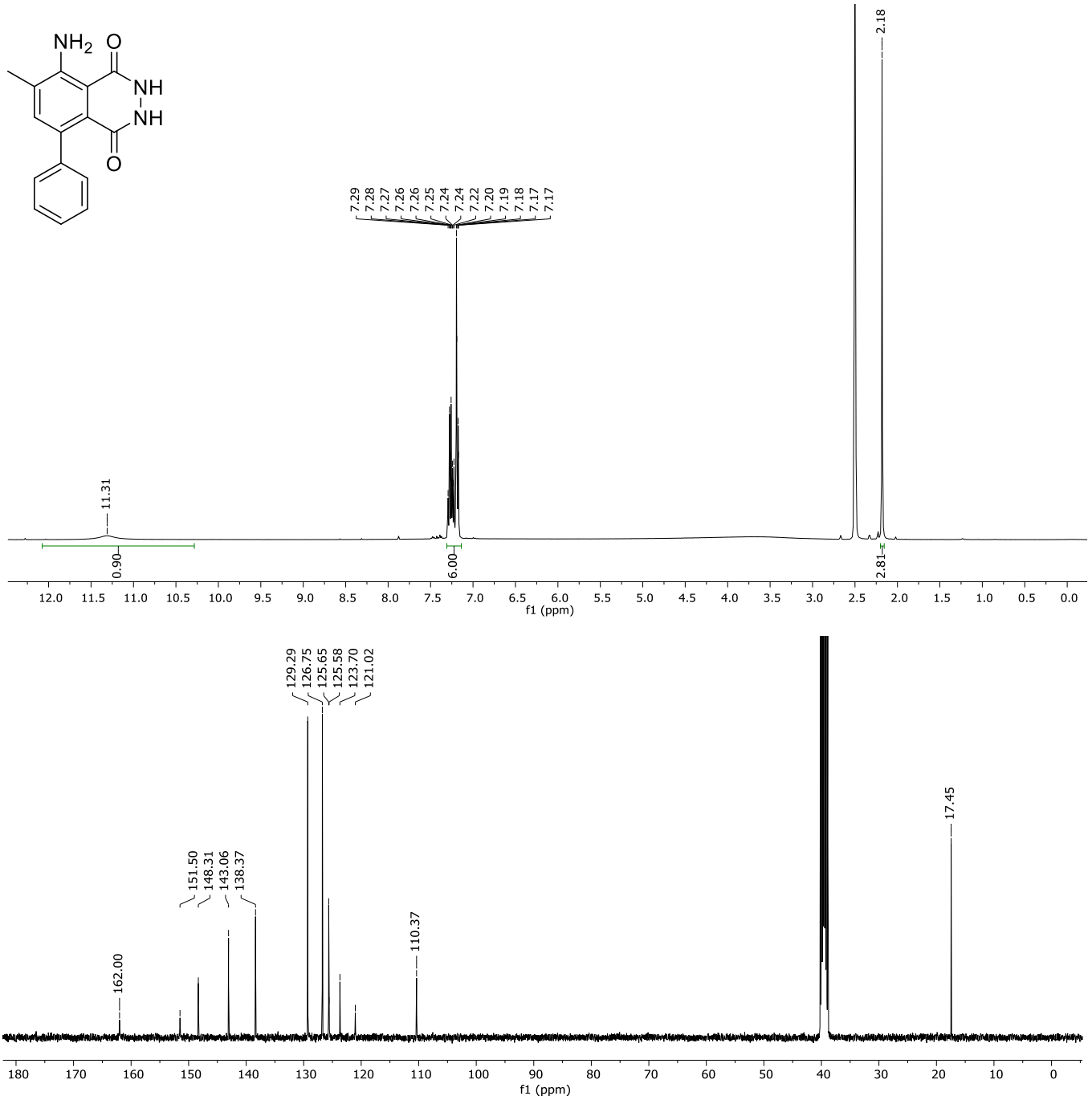

Figure S26. ^{1}H (400 MHz, up) and ^{13}C (101 MHz, down) NMR (DMSO-d_6) spectra of **8h**.

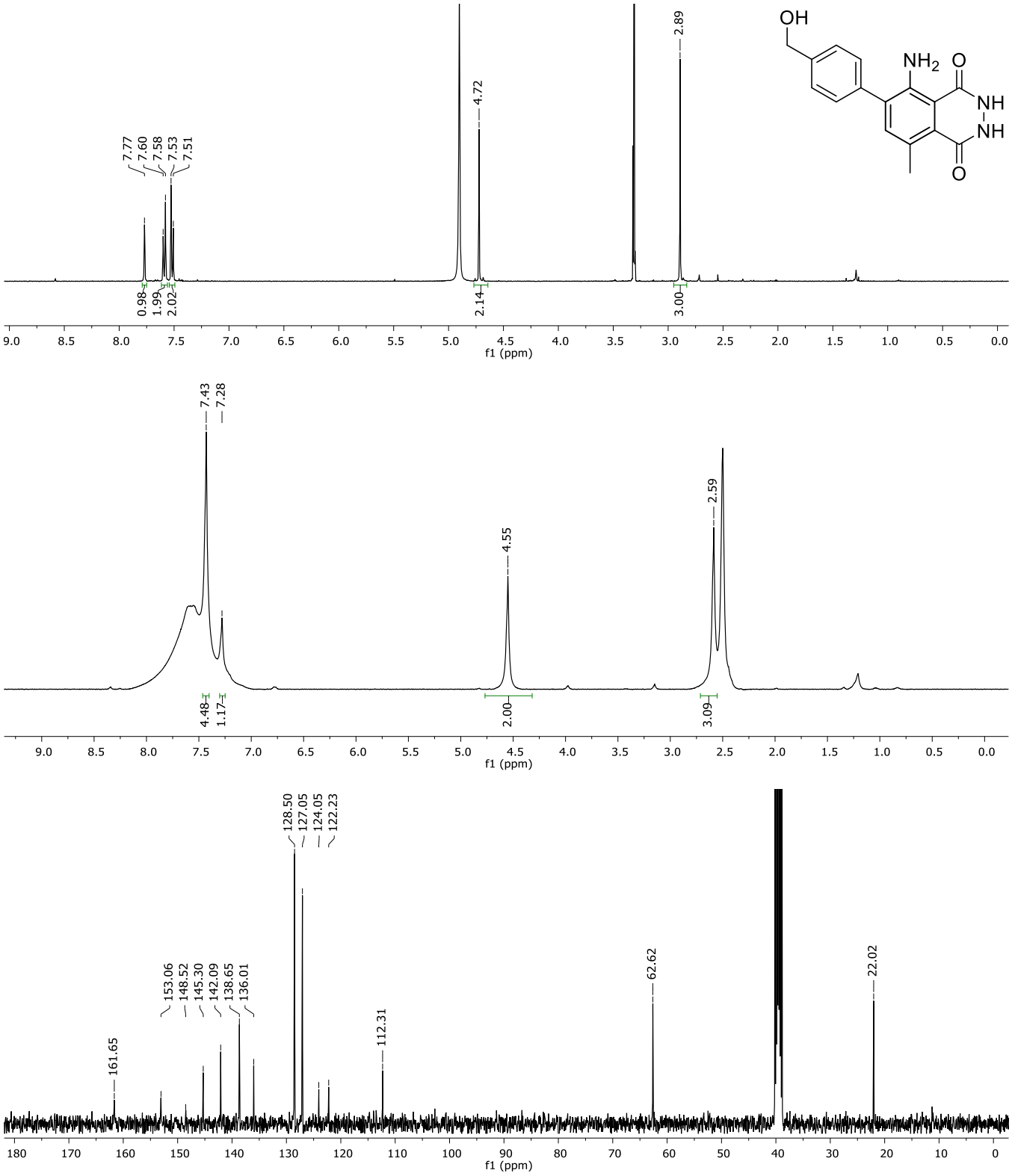

Figure S27. ^{1}H (400 MHz, MeOD-d_4, top), ^{1}H (400 MHz, DMSO-d_6, middle), and ^{13}C (100 MHz, DMSO-d_6, bottom) NMR spectra of **8i**.

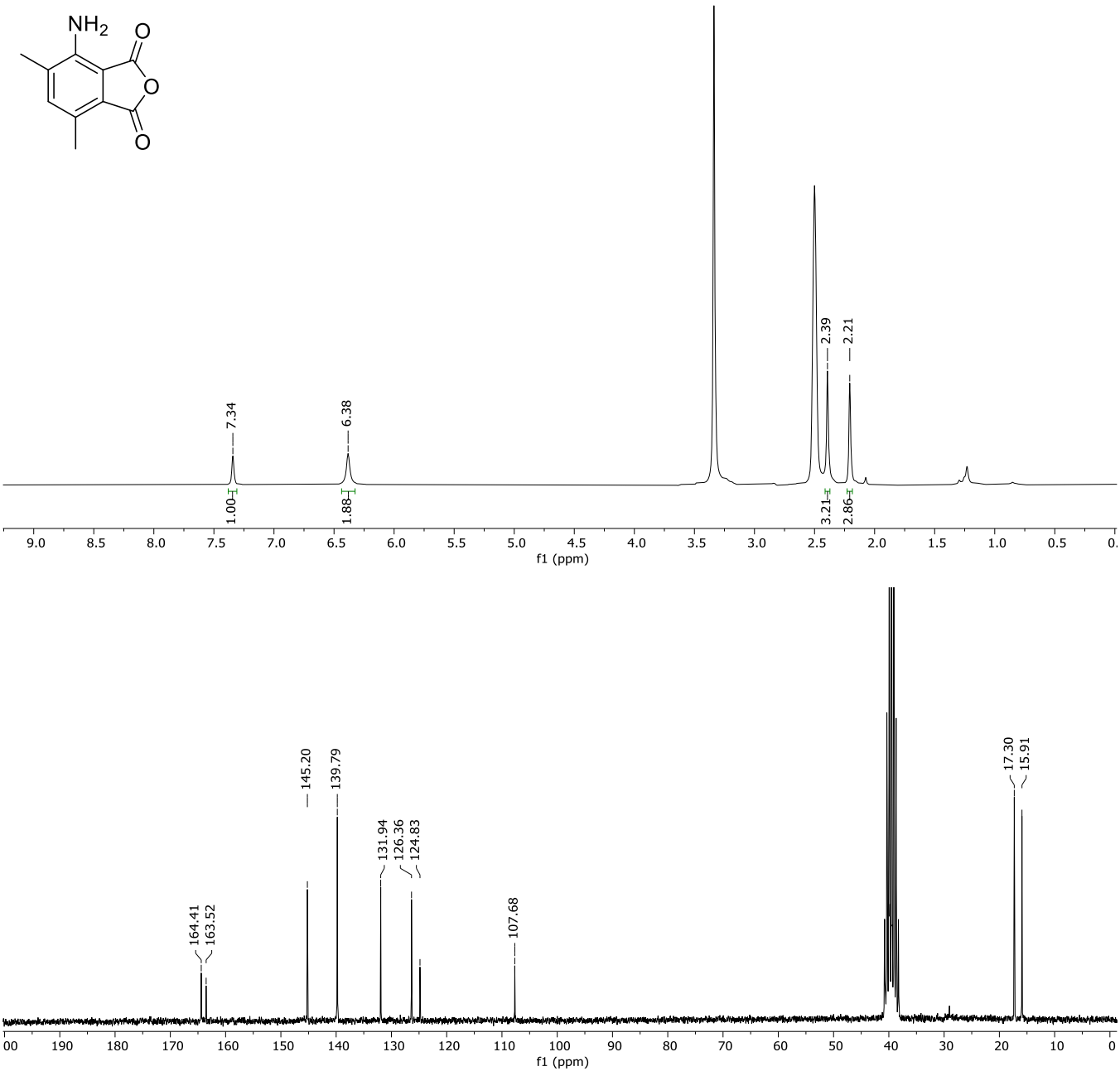

Figure S28. ^{1}H (200 MHz, up) and ^{13}C (50 MHz, down) NMR (DMSO-d_6) spectra of **9a**.

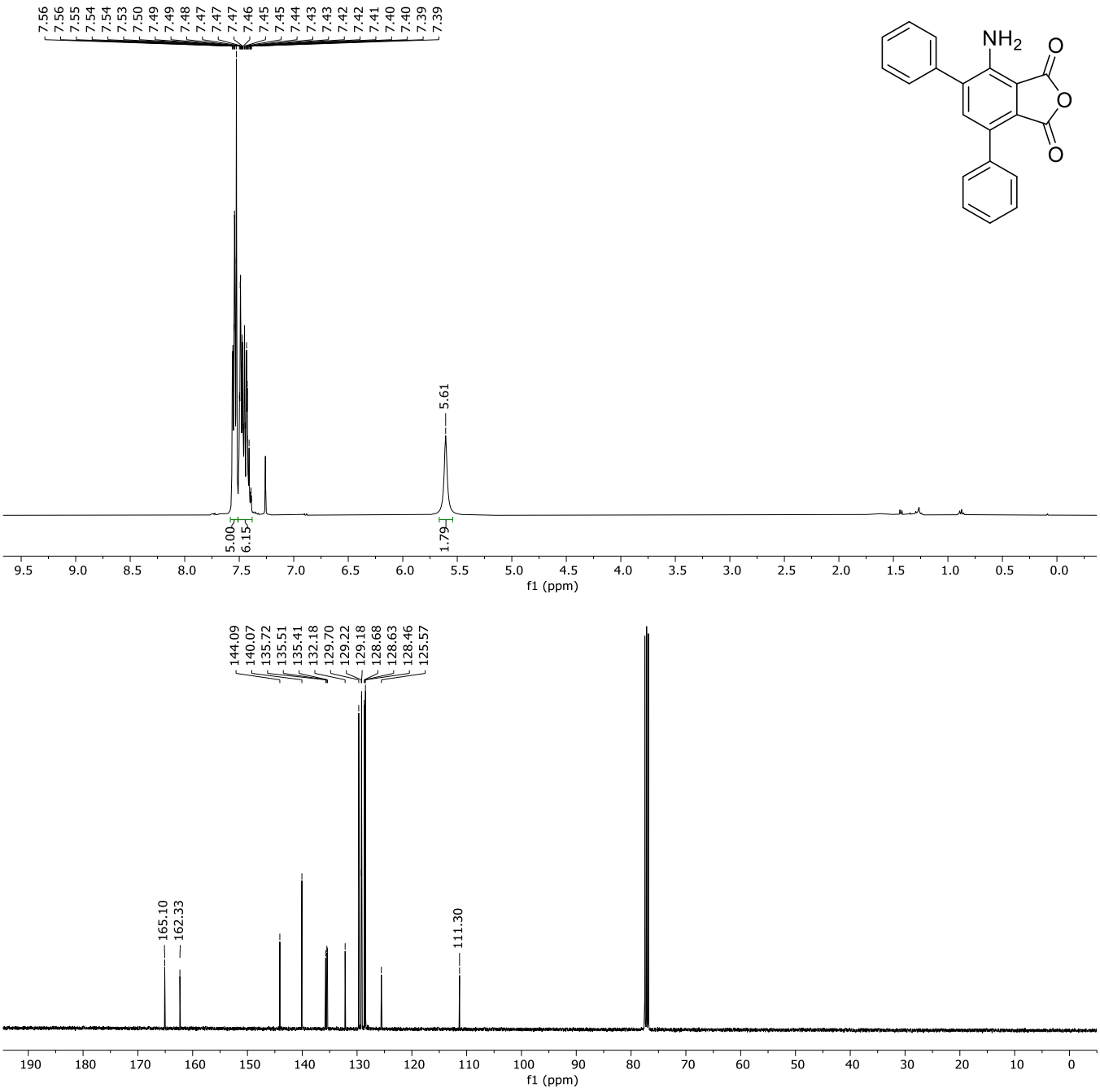

Figure S29. ^{1}H (400 MHz, up) and ^{13}C (101 MHz, down) NMR ($CDCl_3$) spectra of **9b**.

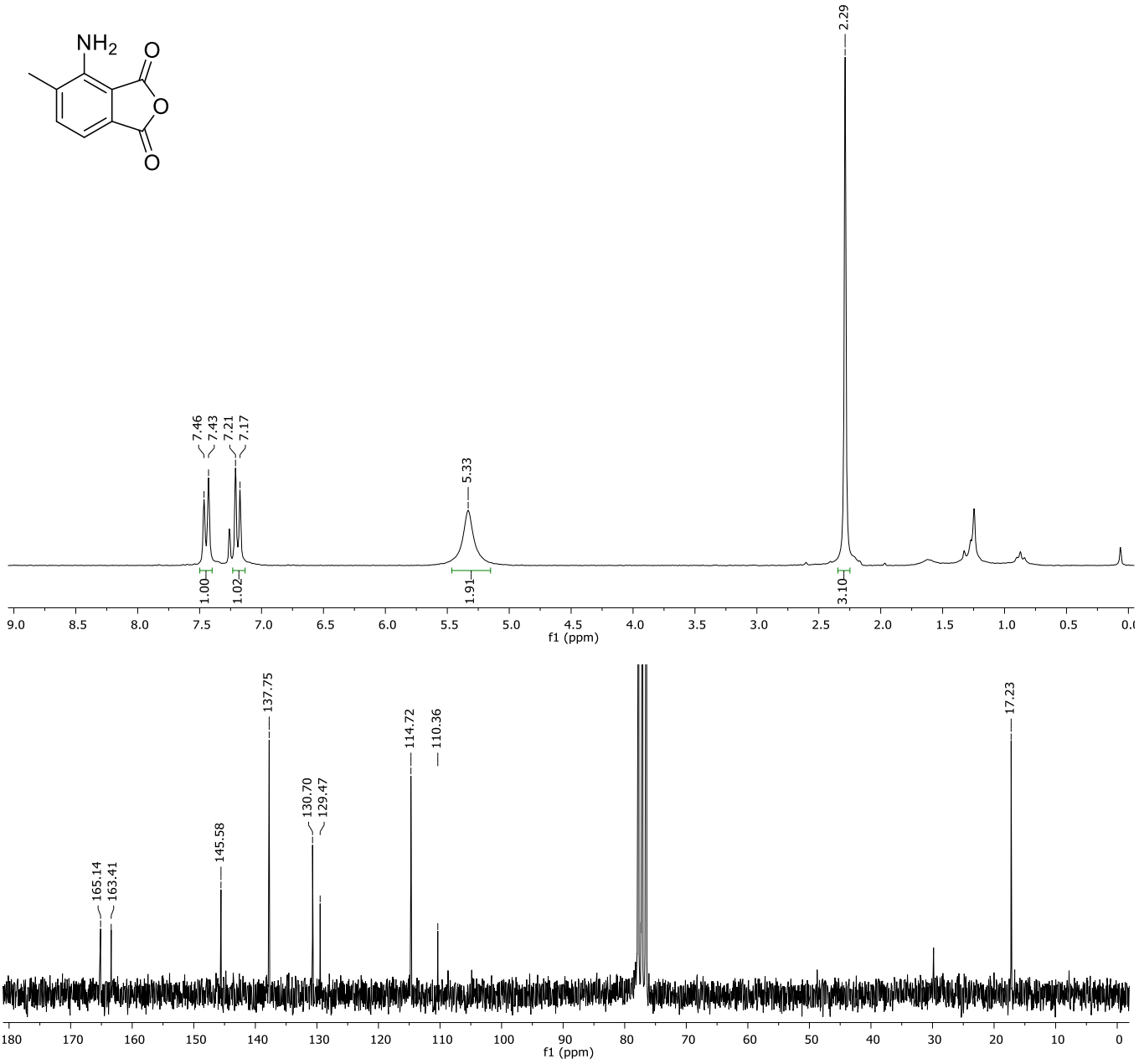

Figure S30. ^{1}H (200 MHz, up) and ^{13}C (50 MHz, down) NMR ($CDCl_3$) spectra of **9c**.

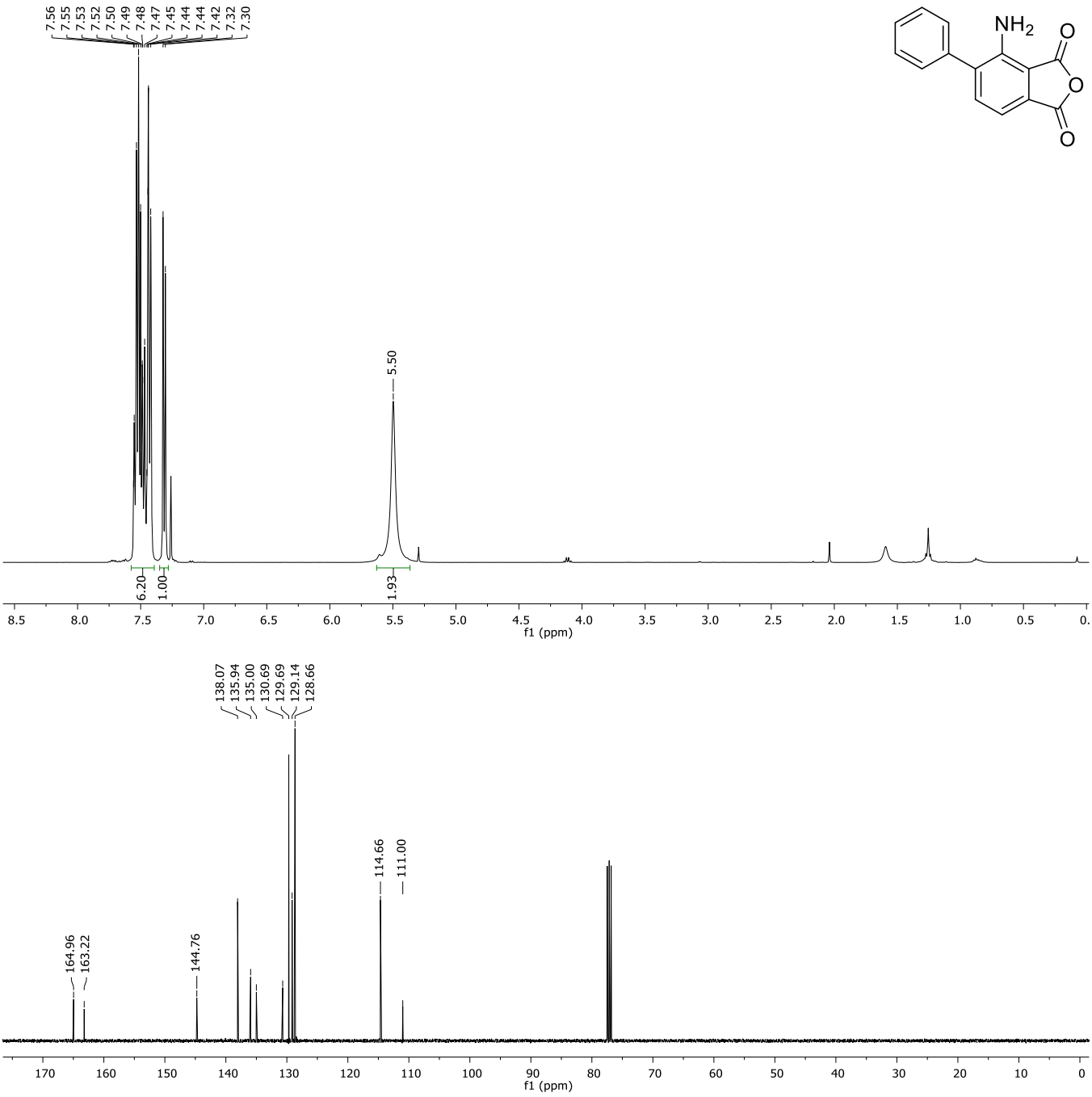

Figure S31. ^{1}H (400 MHz, up) and ^{13}C (101 MHz, down) NMR ($CDCl_3$) spectra of **9d**.

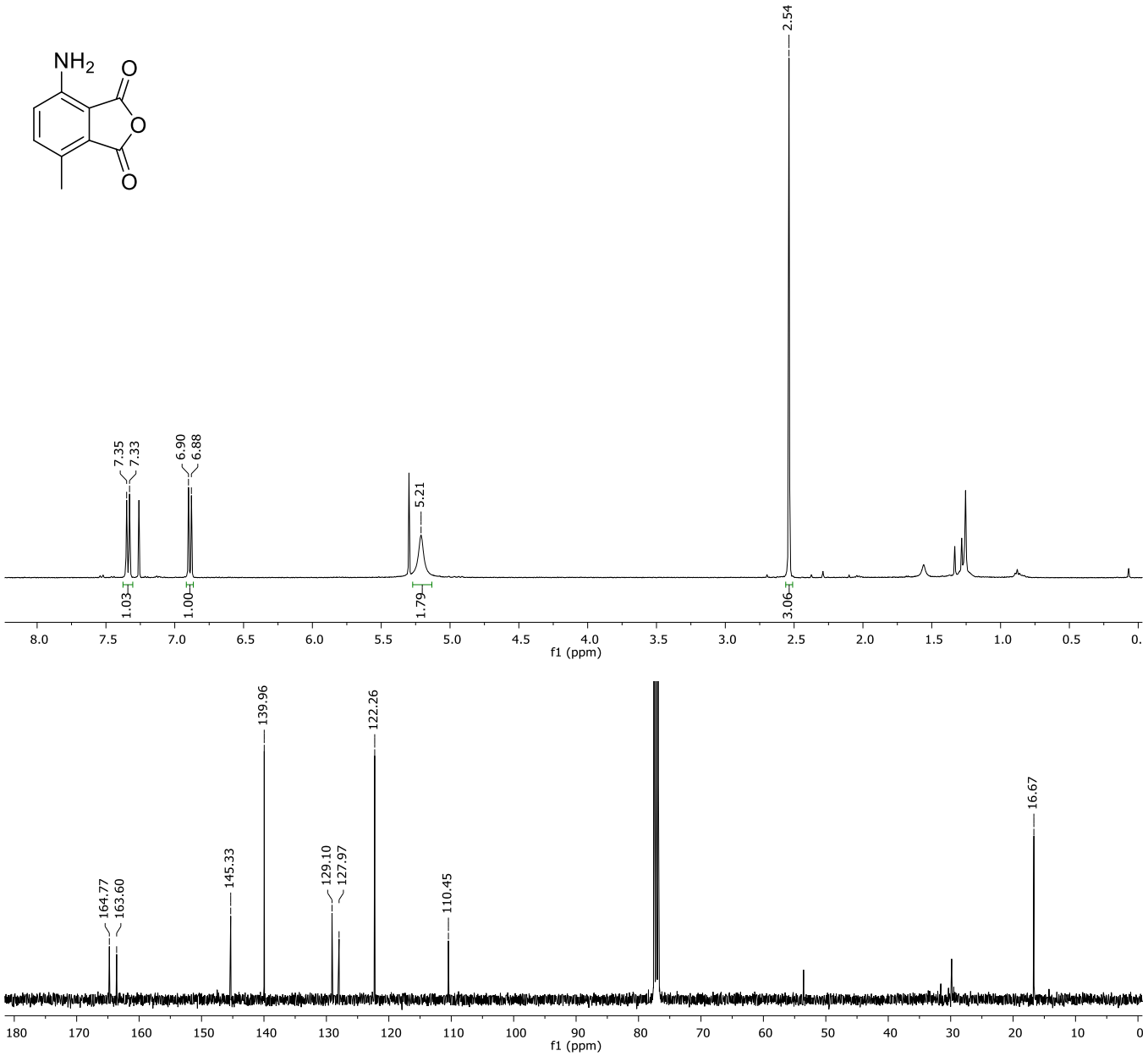

Figure S32. ^{1}H (400 MHz, up) and ^{13}C (101 MHz, down) NMR ($CDCl_3$) spectra of **9e**.

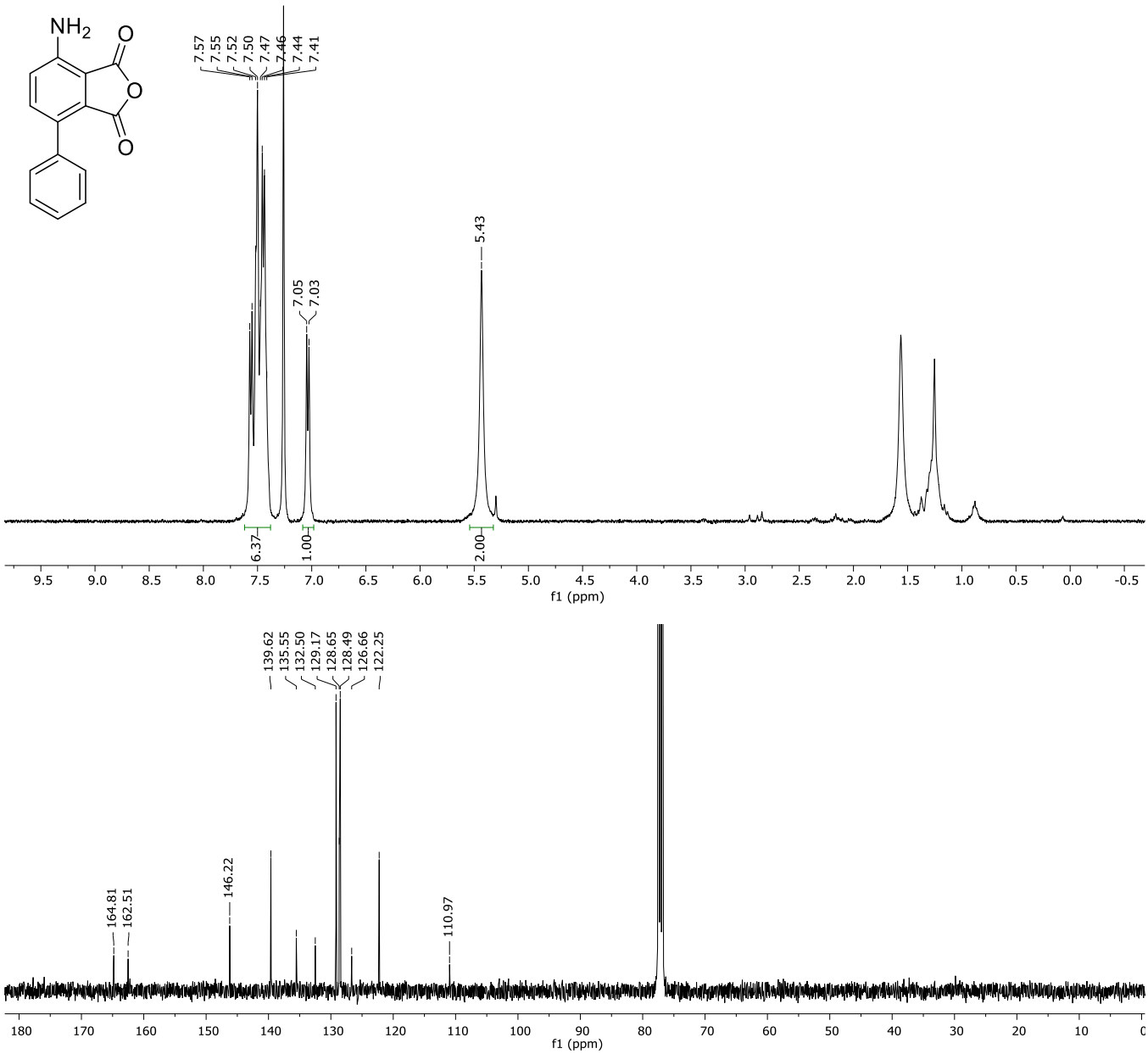

Figure S33. ^{1}H (400 MHz, up) and ^{13}C (101 MHz, down) NMR ($CDCl_3$) spectra of **9f**.

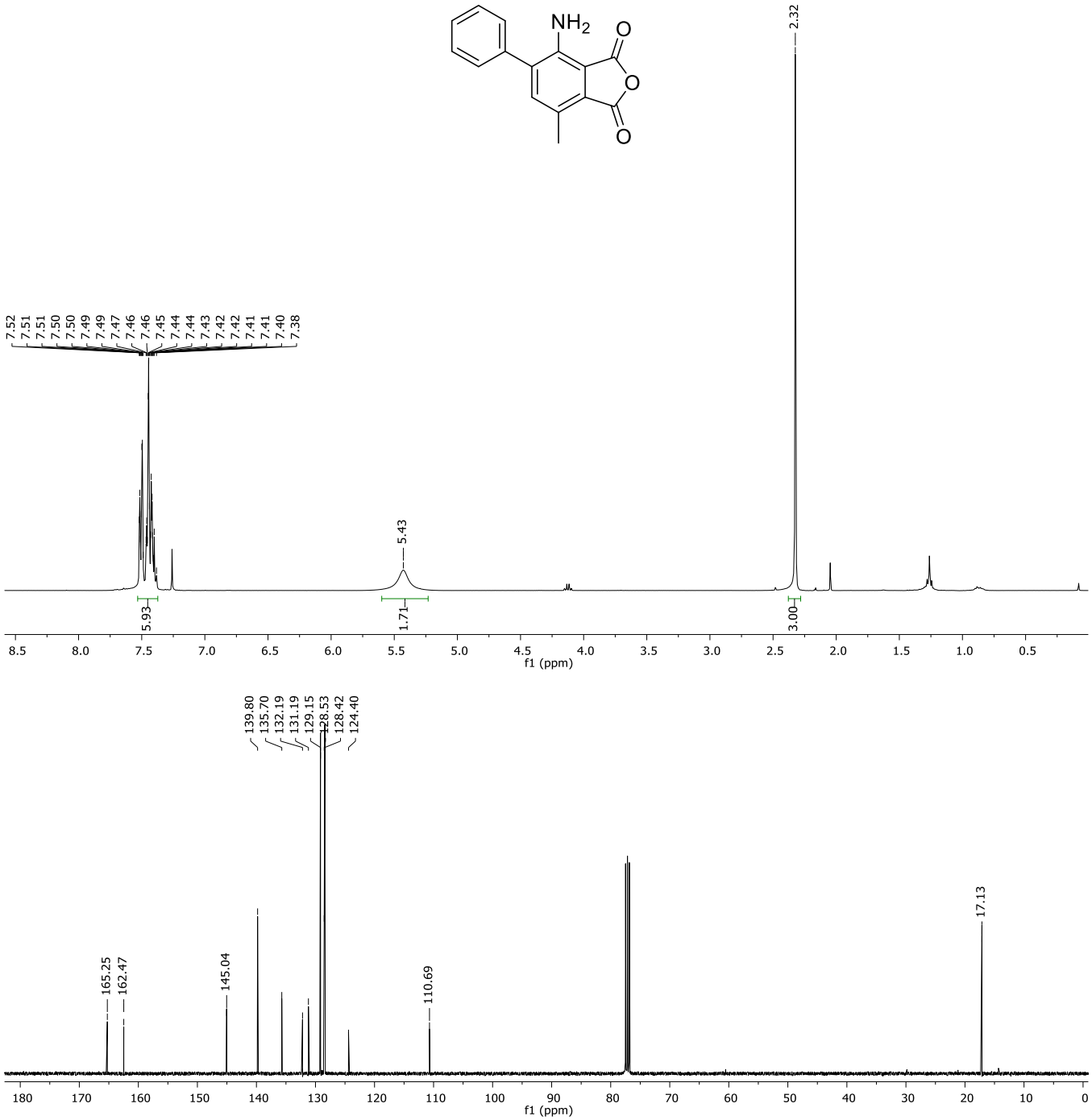

Figure S34. ^{1}H (400 MHz, up) and ^{13}C (101 MHz, down) NMR ($CDCl_3$) spectra of **9g**.

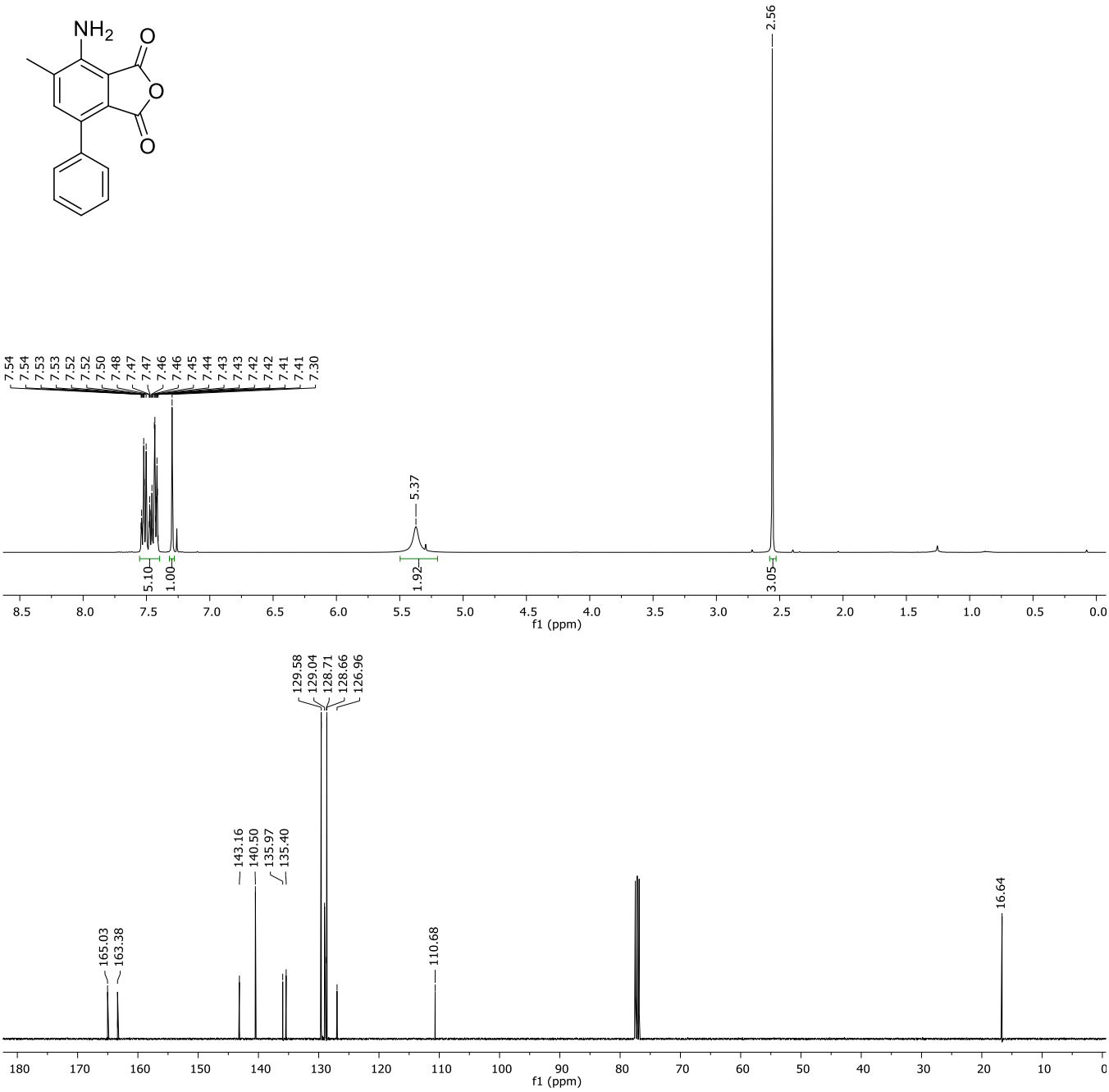

Figure S35. ^{1}H (400 MHz, up) and ^{13}C (101 MHz, down) NMR ($CDCl_3$) spectra of **9h**.

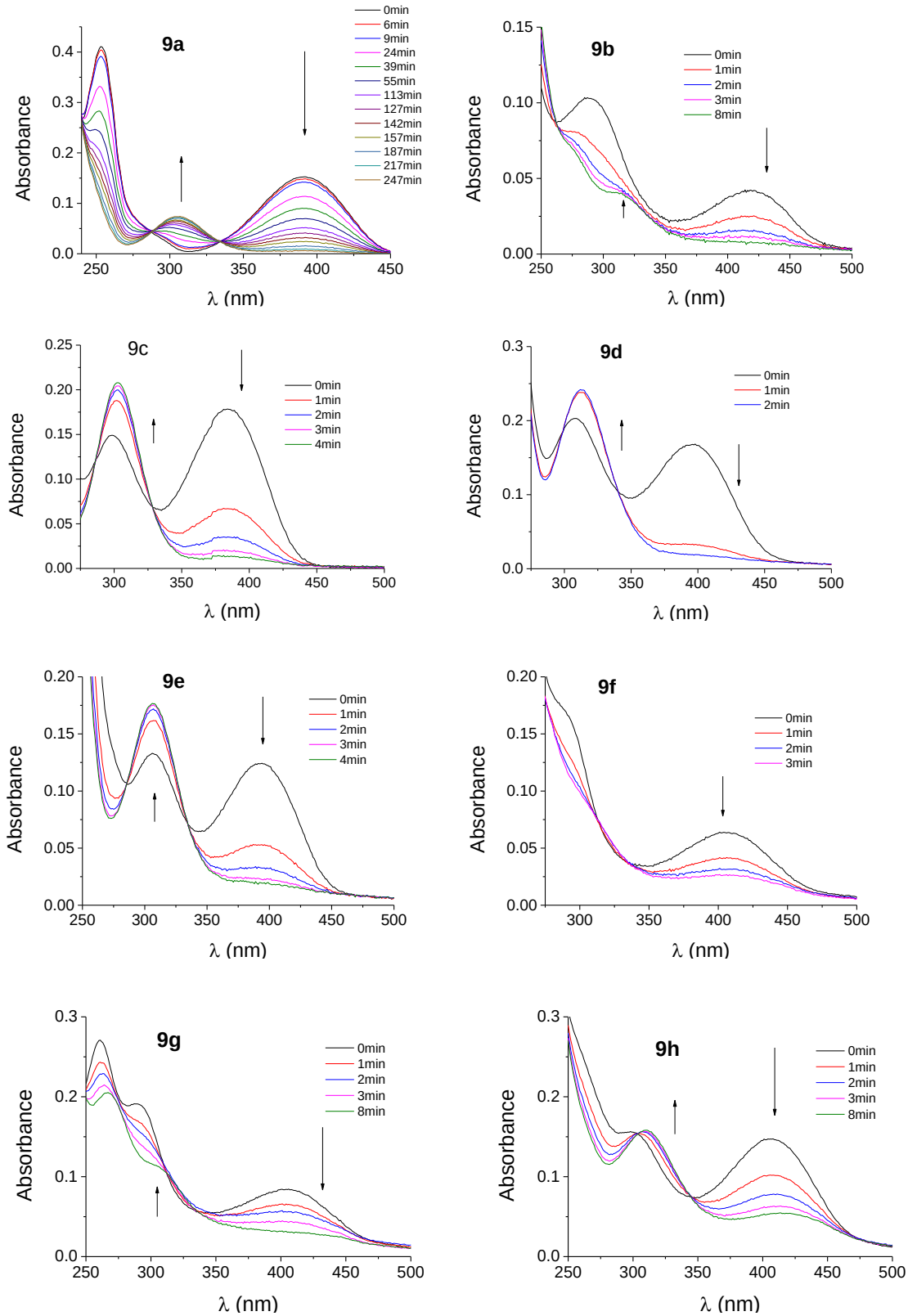

Figure S36. Hydrolysis of the phthalic acid anhydrides yielding the corresponding phthalates **9a-h** in aqueous alkaline media monitored by UV spectroscopy.

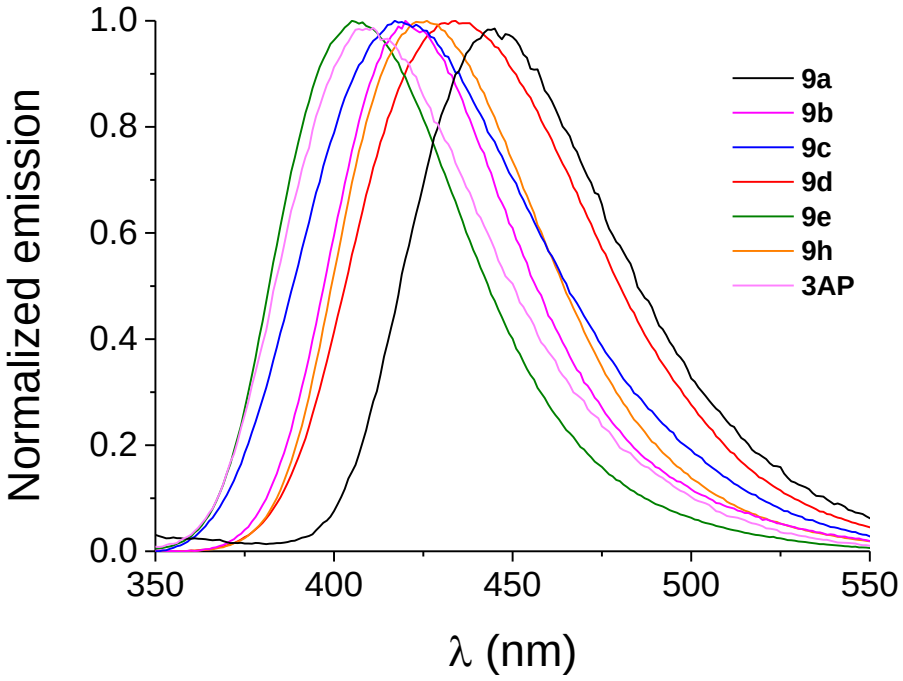

Figure S37. Normalized fluorescence spectra corresponding to phthalates **9a-e**, **9h** and **3AP** in basic aqueous solution (pH 10, λ_{exc} = 310 nm, A (310 nm) = 0.1 for each sample).

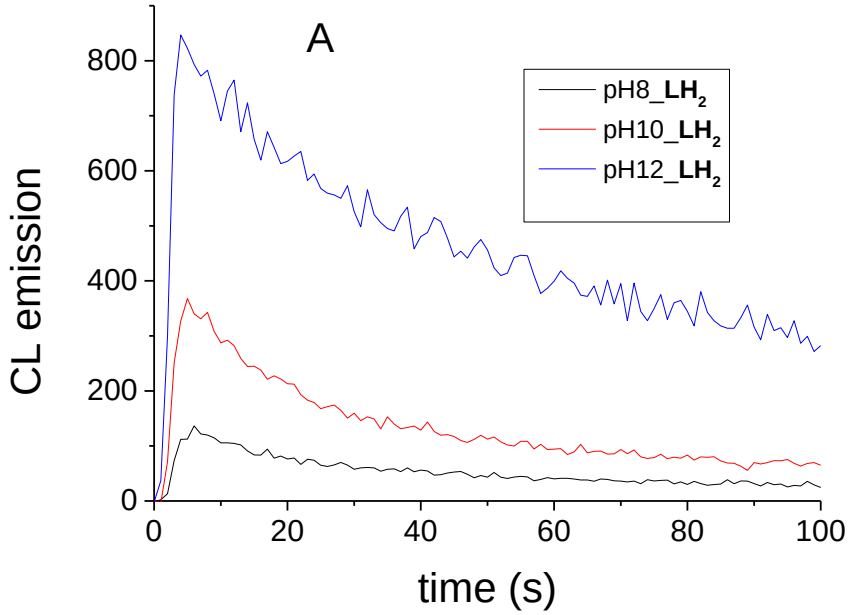

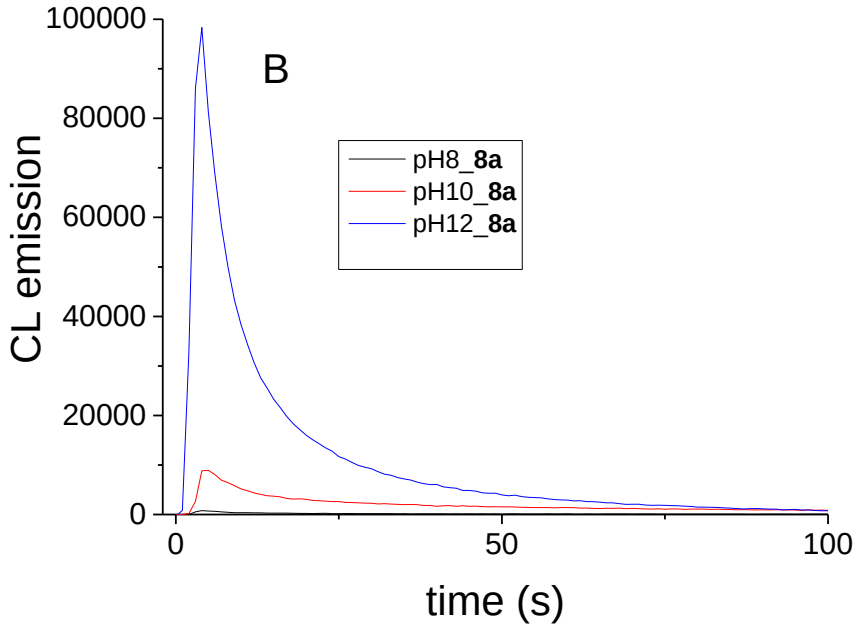

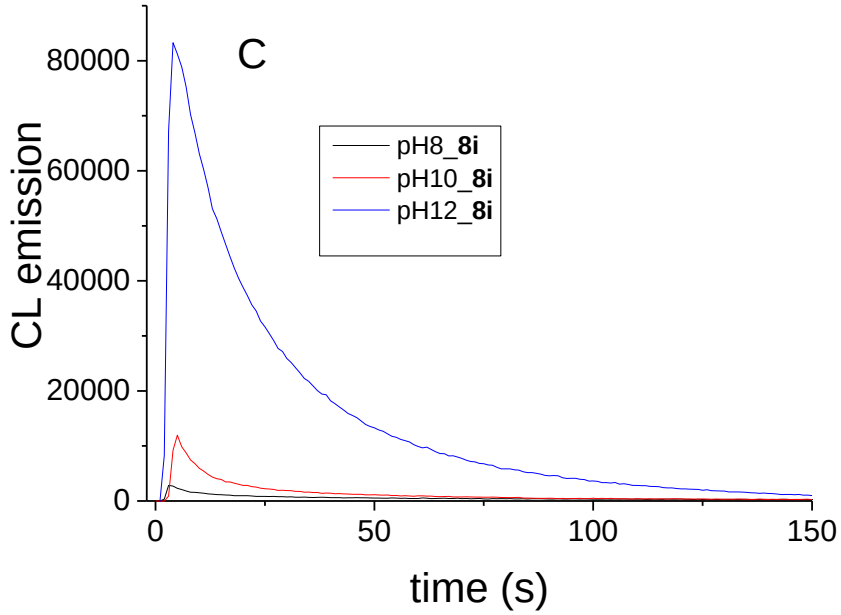

Figure S38. Typical chemiluminescence kinetics displayed by luminol (LH_2, A) and its derivatives **8a** (B) and **8i** (C) in aqueous solutions at different pH: pH= 8, pH= 10 and pH= 12.

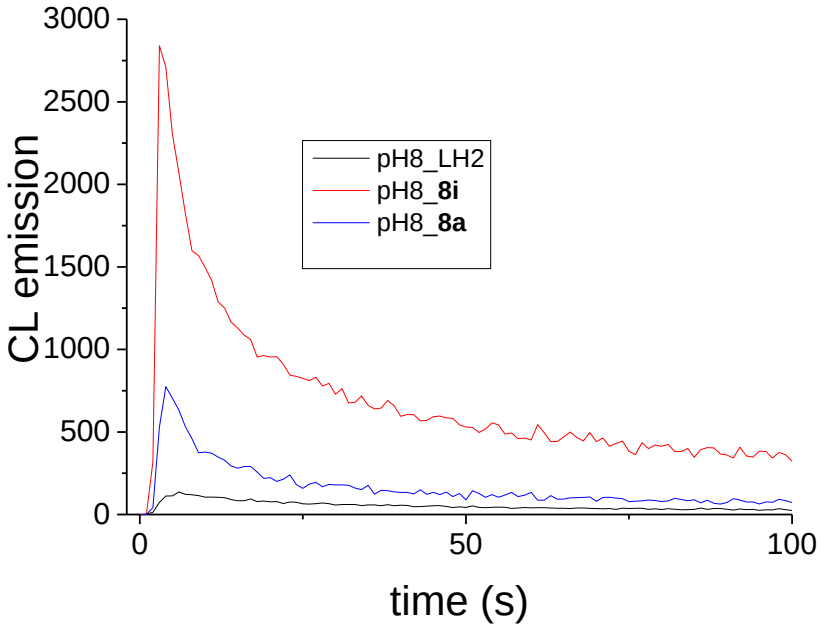

Figure S39. Typical chemiluminescence kinetics displayed by luminol (LH_2), and its derivatives **8a** and **8i** in aqueous solutions at pH=8.

Table S1. Energy barrier between **CP**$^{-2}$ and **TS** ($\Delta E^{\ddagger}$, in eV) of luminol derivatives **8** computed in the gas phase, DMSO solution, and water solution.

Compound	Gas phase	DMSO	water
Luminol	0.17	0.14	0.14
8c	0.18	0.14	0.14
8d	0.24	0.17	0.16
8f	0.22	0.22	0.22
8h	0.23	0.23	0.23
8b	0.26	0.24	0.24
8e	0.2	0.17	0.17
8a	0.22	0.18	0.18
8g	0.26	0.2	0.2